RESEARCH DEPARTMENT

Methods for shaping the vertical radiation patterns of v.h.f. and u.h.f. transmitting aerials

TECHNOLOGICAL REPORT No. RA-10

UDC 621.396.677.31 1967/61

THE BRITISH BROADCASTING CORPORATION
ENGINEERING DIVISION

RESEARCH DEPARTMENT

METHODS FOR SHAPING THE VERTICAL RADIATION PATTERNS OF V.H.F. AND U.H.F. TRANSMITTING AERIALS

Technological Report No. RA-10
UDC 621.396.677.31 1967/61

P.C.J. Hill, Ph.D., B.Sc., D.I.C., C.Eng., M.I.E.E.

D. Maurice
for Head of Research Department

This Report is the property of the British Broadcasting Corporation and may not be reproduced in any form without the written permission of the Corporation.

This Report uses SI units in accordance with B.S. document PD 5686.

Technological Report No. RA-10

METHODS FOR SHAPING THE VERTICAL RADIATION PATTERNS OF V.H.F. AND U.H.F. TRANSMITTING AERIALS

Section Title Page

SUMMARY 1

LIST OF PRINCIPAL SYMBOLS 1

1. INTRODUCTION 1

2. GENERAL CONSIDERATIONS 3

2.1. Theoretical 3
2.2. Practical 3

3. TECHNIQUES FOR SYNTHESIZING NULL-FILLED PATTERNS 4

3.1. Constant-Phase Solutions 4
    3.1.1. Unequal Power Division 4
    3.1.2. Twin-Beam Method 5
3.2. Constant-Amplitude Solutions 7
    3.2.1. Phase Perturbation 7
    3.2.2. Stationary-Phase Method 8
3.3. Variable Amplitude-and-Phase Solutions 9
    3.3.1. Central-Tiers Method 10
    3.3.2. Woodward's Cosecant Solution 10
    3.3.3. Current Perturbation ('Woodward-Quadrature') 12
    3.3.4. General Stationary-Phase Methods 12
    3.3.5. Polynomial-Root Perturbation 14
3.4. Further Synthesis Solutions for Design Optimization 15

4. APPLICATION TO PRACTICAL TRANSMITTING AERIALS 16

4.1. Aerials with Individually-Fed Tiers 17
4.2. Panel-Aerials 18
    4.2.1. General Considerations 18
    4.2.2. Design Examples 19
4.3. Aerial Impedance Compensation 24
4.4. Practical Limitations 25

5. FINAL REMARKS AND CONCLUSIONS 26

6. REFERENCES 27

December 1967

Technological Report No. RA-10
UDC 621.396.677.31 1967/61

METHODS FOR SHAPING THE VERTICAL RADIATION PATTERNS OF V.H.F. AND U.H.F. TRANSMITTING AERIALS

SUMMARY

An important problem in the design of v.h.f. and u.h.f. transmitting aerials is the provision of a vertical radiation pattern which gives approximately uniform field strength over the prescribed service area. A good solution is provided by a beam-tilted cosecant-shaped radiation pattern. Several methods are described for synthesizing radiation patterns of this type by varying either the amplitudes or the phases (or both) of the radiating currents in a linear column of equispaced elements. Some examples are given of the application of these techniques to the types of multi-tiered aerials employed at v.h.f. and u.h.f. broadcast stations. Consideration is also given to the problems of realizing the required current distributions, and important design factors such as aerial impedance matching, gain reduction and pattern bandwidth are discussed. Finally the various pattern shaping solutions are briefly compared.

PRINCIPAL SYMBOLS

$2a$	change of amplitude with unequal power division
A_r	point-source amplitude distribution
$A(x)$	continuous amplitude distribution
b	height of pedestal distribution
c	current amplitude in central tier(s)
d	source spacing (wavelengths)
f	frequency
G	aerial gain (dB)
G_0	reference gain of uniformly fed aerial (dB)
I_r	point-source current distribution ($= A_r \exp(\mathrm{j}\phi_r)$)
$I(x)$	continuous current distribution ($= A(x) \exp\{\mathrm{j}\phi(x)\}$)
k	magnitude of radiation pattern
m_q	null-filling index at the qth null-point
N	length of array (wavelengths); number of sources
$p(s), P(\theta)$	radiation pattern functions
q	null-point number
r	source number
R_q	amplitude of the qth root of array polynomial ($= \lvert z_q \rvert$)
s	pattern variable ($= \sin\theta$)
x	distance along array (wavelengths)
z	polynomial variable ($= R \exp(\mathrm{j}\psi)$)
α	value of x at point of 'stationary-phase'
2Δ	differential phase-shift
θ	declination angle
θ_0	beam-tilt angle
λ	wavelength
ρ	reflexion coefficient of dipole or panel
ρ_{in}	net input reflexion coefficient
ϕ_r	point-source phase distribution
$\phi(x)$	continuous phase distribution
Φ_r	phase distribution for panels
ψ	parameter defined by $\psi = \pi N d s$

1. INTRODUCTION

An ideal broadcast service provides uniform average field strength at all distances up to the limit of the service area. Practical aerials cannot easily satisfy this requirement in the more distant parts of the service area because path attenuation increases rapidly as the horizon is approached. It is possible, however, to shape the vertical radiation pattern (v.r.p.) of a multi-tiered aerial in order to achieve approximately uniform field strength near to the transmitter; this is particularly practicable at u.h.f. where the average received field strength is approximately equal to that of the direct wave because local ground irregularity greatly reduces the contribution from the ground-reflected wave. Uniform direct-wave field strength is then obtained by making the amplitude of the v.r.p. of the transmitting aerial proportional to cosec θ where θ is the declination angle from the horizontal. In practice, the main beam of the v.r.p. is tilted downwards by a small angle θ_0 corresponding to the limit of the service area, in order to prevent power being wasted above the horizon.

The simplest form of transmitting aerial consists of a vertical array of, typically, 8 to 40 similar tiers of equi-spaced elements, each carrying equal co-phased currents. The v.r.p. of such an arrangement is given by

$$P(\theta) = \frac{\sin(\pi Nd\ \sin\theta)}{N\sin(\pi d\ \sin\theta)} \qquad (1)$$

where N is the number of elements spaced d wavelengths apart, the pattern having been normalized by setting the amplitude of the main beam $P(0)$ to unity. It is important to note that for an inter-tier spacing not exceeding one wavelength (1·0λ) the v.r.p. in the important region $0<\sin\theta<0{\cdot}5$ is approximately identical to the pattern from a uniformly illuminated aperture Nd wavelengths long, i.e.

$$P(\theta) \simeq \frac{\sin\psi}{\psi} \qquad (2)$$

where $\psi = \pi Nd\ \sin\theta$. The magnitude of this pattern $|P(\theta)|$ is plotted as a function of ψ in Fig. 1(*a*). The envelope of the curve is given by $1/\psi$ and since this is proportional to cosec θ it follows that the envelope represents the v.r.p. which gives uniform field strength in the nearer parts of the service area. Thus, if the pattern can be re-shaped between its sidelobes by filling in the nulls to approach the cosecant envelope, the v.r.p. would become satisfactory. This process will be referred to as 'null-filling' and, as with any pattern shaping, it requires a departure of the aerial current distribution from the uniform co-phased condition.

The v.r.p. which is required for a broadcasting service is one which is beam-tilted and null-filled below the horizontal. Practical current distributions provide only an approximation to the cosecant v.r.p. and it is therefore desirable to specify upper and lower amplitude bounds for the null-filled pattern. A convenient expression for the pattern bounds is as follows:

$$|P(\theta)| = \frac{m\hat{P}\ \text{cosec}\ (\theta - \theta_0)}{\pi Nd} \qquad [\theta_1 \leqslant \theta - \theta_0 \leqslant \theta_2] \qquad (3)$$

where $\hat{P}$ is the amplitude of the main lobe, θ_0 the beam-tilt angle and m defined as the null-filling index*; θ_1 and θ_2 are the angular limits of the pattern specification. The significance of the index m is best understood by observing that the sidelobe envelope of the uniformly illuminated aperture is given by $(1/\pi Nd)$ cosec θ; this envelope corresponds to a null-filling index $m = 1{\cdot}0$. This is illustrated in Fig. 1(*b*) which shows idealized beam-tilted v.r.p.s with null-filling below the horizontal corresponding to $m = 0{\cdot}5$ (50%) and $m = 1{\cdot}0$ (100%); the broken curve is the v.r.p. of the equivalent uniformly-fed aperture. The v.r.p. of a practical u.h.f. (main-station) aerial should typically satisfy the following specification:

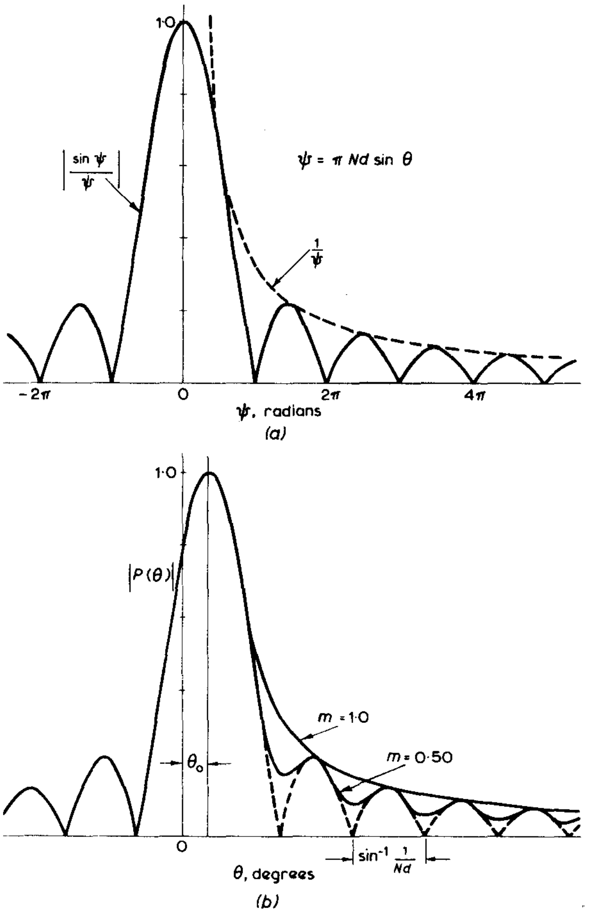

Fig. 1 - Illustrating vertical radiation pattern shaping by null-filling

(*a*) Vertical radiation pattern of a uniform aperture
(*b*) Idealized vertical radiation patterns with beam-tilt θ_0 for a linear array of N sources spaced d wavelengths apart

upper bound, $m = 1{\cdot}25$ $\quad \sin^{-1}(1/Nd) \leqslant \theta - \theta_0 \leqslant 25°$

lower bound, $m = 0{\cdot}70$ $\quad \sin^{-1}(1/Nd) \leqslant \theta - \theta_0 < 10°$

$m = 0{\cdot}50$ $\quad 10° < \theta - \theta_0 \leqslant 25°$

the lower limit in each case being the declination of the first pattern null-point. No null-filling is required above the horizontal (θ negative in Fig. 1(*b*)) and it is desirable to keep the upper sidelobes as small as possible to avoid excessive gain-reduction; it is not always practicable, however, to control the pattern shape in this region.

The v.r.p. of an aerial is determined by the amplitude and phase distribution of current over the tiers together with the inter-tier spacings. The pattern can be shaped by varying these parameters, either singly or in combination, from the uniform condition. The difficulties which arise in such pattern synthesis are both fundamental and practical. On the theoretical side the major problems are that the current distribution must be made to fit the the dimensions of the aperture and also that the phase variation of the radiation pattern is arbitrary. In practice there is only a finite number of tiers available so that the main difficulty in realizing the required pattern results from the limited number of source currents which can be independently controlled and also from the necessity of feeding the aerial tiers through a practical power-splitting arrangement. A further important practical requirement is that the current distribution should not vary appreciably with frequency and should lead to acceptable figures for aerial impedance and gain; a subsidiary requirement is that each half of the aerial should have a v.r.p. which is satisfactory for emergency use.

---

* 100m is often referred to as the 'percentage null-filling'.

In this report we describe and compare a variety of methods for null-filling (or cosecant-shaping) the v.r.p.s of v.h.f. and u.h.f. aerials. At v.h.f., fewer tiers are used and broad main lobes result; consequently beam-tilt is seldom necessary and null-filling is only required if the aerial is situated near a built-up area. Although most of the synthesis methods described are equally valid for v.h.f. and u.h.f. aerials, emphasis is placed on their application to u.h.f. aerials throughout the report.

2. GENERAL CONSIDERATIONS

The more important general theoretical and practical aspects of pattern synthesis relevant to null-filling aerial v.r.p.s are now outlined prior to the formal descriptions of the various available techniques.

2.1. Theoretical

We start by considering a linear array of N isotropic sources with an aperture distribution given by $I_r = A_r \exp(j\phi_r)$ where A_r and ϕ_r are the amplitude and phase respectively of the current in the rth source. The complex radiation pattern $p(\sin\theta)$ of the array may be written

$$p(\sin\theta) = \sum_{r=0}^{N-1} I_r \exp(-j2\pi r d \sin\theta) \qquad (4)$$

where rd is the distance of the rth source from the point of phase reference with d the 'fundamental' source-spacing in wavelengths (λ). Since I_r is the complex Fourier line spectrum of the pattern function $p(\sin\theta)$, the formal solution to pattern shaping problems is given by the inverse integral transform of Equation (4). The complex pattern repeats every $1/d$ in $\sin\theta$ and for fixed source spacings its control is confined to this range through the $2N-1$ degrees of freedom within I_r. The accuracy with which a pattern may be synthesized can be increased for a given aperture by increasing N and reducing d. If d is less than 0·5, however, part of the pattern over which control is unavoidably exercised falls within the imaginary region $|\sin\theta| > 1$. This means that the limiting accuracy of a synthesized pattern is set by the amount of reactive energy which can be tolerated within the aperture[1]; moreover, in practice, mutual coupling between sources precludes accurate realization of a very closely spaced array.

Direct inversion of Equation (4) is impossible in all but a few special cases because we are concerned only with the power pattern $|p(\sin\theta)|^2$ and also because the size of the aperture ($Nd\lambda$) is limited. A powerful method for circumventing these difficulties is to synthesize the required pattern or pattern component by the superposition of a set of orthogonal, 'aperture-limited', and co-phased pattern functions. Many of the null-filling techniques to be described use the best-known example of these functions for synthesis; this is the Woodward 'sinc' function[2] which is simply the radiation pattern of a uniformly-fed aperture* (c.f. Equation (2)). Two other general synthesis techniques to be employed deal directly with the power pattern. The first is based on an asymptotic evaluation of the integral expression for the pattern of a large continuous array[3,4,5] and the second is based on the polynomial representation of a discrete array[6]; both these methods may be used for finite apertures. Another approach is to use variational methods[7,8] but the disadvantage is that rather arbitrary decisions must be taken at the outset; these methods have not been pursued here in view of the simpler explicit solutions which have been developed. Most of the solutions to be adopted are essentially of the null-filling type, the remainder being based on actual cosecant-pattern shaping.

It is usually more convenient, if not necessary, to synthesize from a continuous aperture and then to sample the resulting current distribution at the positions of the sources in the practical aerial under consideration. Beam-tilt is inserted into the pattern by superposing an appropriate linear phase progression on to the aerial current distribution.

2.2. Practical

Practical v.h.f. and u.h.f. transmitting aerials are sectionalized and fed from one (or more) transmitters through power-splitting devices, the individual tiers being energized via local groups of branch feeders. The variables available for pattern shaping and null-filling are the spacings of the sources and the amplitudes and phases of their currents. Phase variation can be achieved by adjusting the lengths of the branch feeders whereas amplitude variation requires the complication of current transformers. It follows that the preferred arrangements of sources in order of practical complexity is:

---

* The sinc function is defined by $\text{sinc}\, x = \dfrac{\sin \pi x}{\pi x}$

(a) Equally spaced sources or tiers carrying currents of equal amplitude but arbitrary phase (constant-amplitude solution)

(b) Unequally spaced sources carrying equal cophased currents (constant-current solution)

(c) Unequally spaced sources with currents of equal amplitude but arbitrary phase

(d) Equally spaced sources with currents of arbitrary amplitude but equal phase (constant-phase solution)

(e) Unequally spaced sources with currents of arbitrary amplitude but equal phase

(f) Equally spaced sources with currents of arbitrary amplitude and phase (complex-current solution)

(g) Unequally spaced sources carrying arbitrary currents

It turns out that unequally spaced sources are unattractive because they generally lead to inefficient utility of the aerial aperture and some of the source-spacings required are too small to be practicable. Consequently solutions of the types (b), (c), (e) and (g), will not be considered here; the preferred solutions now become, in order of preference,

(i) constant amplitude, A_r

(ii) constant phase, ϕ_r

(iii) complex current (variable amplitude and phase)

A simple aerial-feeding arrangement, however, will not be the sole criterion in selecting a particular null-filling or pattern-shaping technique since other important factors may predominate. For example, a co-phased distribution provides a symmetrical radiation pattern so that the v.r.p. would be equally null-filled above and below the horizontal, resulting in unnecessary loss of aerial gain. Moreover, where beam-tilt is required, the current distribution must have some phase variation. In addition, if non-uniform null-filling is required, the techniques involving cosecant-pattern shaping are generally inapplicable since they cannot easily be made to control the null-filling independently over selected angular ranges.

Finally, it is worth noting at this stage that as we are only interested in the power pattern, array theory can lead us to many $(2^{N-1} - 1)$ other current distributions which are derivable, in theory at least, from the original distribution[9]; one or more of these distributions may offer significant practical advantages compared with the parent distribution.

3. TECHNIQUES FOR SYNTHESIZING NULL-FILLED PATTERNS

The more important basic procedures for synthesizing null-filled v.r.p.s are described below. For convenience, these techniques are grouped according to the types of current distribution they provide, namely, constant phase, constant amplitude, and variable amplitude and phase. Beam-tilt is omitted at this stage and we consider only arrays of equally spaced isotropic sources. In design examples, the source-spacing is taken as 1·0λ (i.e. $d = 1$) but there is no loss of generality here since the general case is obtained by suitably re-scaling the sin θ axis. In the analysis which follows it will be convenient to write $s = \sin\theta$ for the angular variable.

3.1. Constant-Phase Solutions

Co-phased current distributions produce symmetrical radiation patterns, i.e. $|p(s)| = |p(-s)|$. It follows that constant-phase synthesis methods give v.r.p.s which are null-filled to equal levels above and below the horizontal.

3.1.1. Unequal Power Division

This method of null-filling is often used at v.h.f. In its simplest form, the aerial is split into two equal sections but one half carries a greater power.

The mechanism of null-filling is best understood by splitting the current distribution of the equivalent aperture into its even and odd components; the v.r.p. of the even component is null-filled by the v.r.p. of the odd component, the patterns being in phase quadrature with one another. Suppose we consider an $N\lambda$ co-phased aperture, see Fig. 2(*c*), whose amplitude distribution $A(x)$ is given by $A(x) = 1 + a$ for $0<x<N/2$ and $A(x) = 1 - a$ for $-N/2<x<0$; the power ratio between upper and lower sections is $(1 + a)^2/(1 - a)^2$. The even component is identical to the distribution of a uniform aperture so that the corresponding 'primary' pattern $p_0(s)$ is given by Equation (2) (which is not normalized) which is re-written thus,

$$p_0(s) = N \operatorname{sinc}(Ns) \qquad (5)$$

The nulls in this pattern (Fig. 2(*a*)) occur at declinations given by $Ns = \pm 1,2,3, \ldots$ Fourier transformation of the odd component gives a 'secondary' pattern $p_n(s)$ which can be written,

$$p_n(s) = -\mathrm{j}aN \sin(\pi Ns/2)\ \mathrm{sinc}(Ns/2) \qquad (6)$$

The quadrature pattern of Equation (6) is illustrated in Fig. 2(*b*); it possesses nulls at $Ns = \pm 2,4,6,\ldots$, and an approximate cosecant envelope, $2a/\pi s$. The pattern p_n will therefore null-fill the primary pattern p_0 at the odd null-points $s = \pm 1/N, 3/N, \ldots\ldots$, to a uniform level $m = 2a$. The net v.r.p., given by the complex sum of p_0 and p_n, is shown in Fig. 2(*c*) for the case $a = 0{\cdot}25$, $m = 0{\cdot}50$, i.e. 50% null-filling; this corresponds to a power ratio of 25 : 9. A power ratio of 2 : 1 will provide 34% null-filling at the odd null-points.

Null-filling inevitably reduces the gain of the aerial. The power in the null-filling pattern p_n is proportional to Na^2 and since p_0 and p_n are in phase quadrature, the total power in $p_0 + p_n$ is proportional to $N(1 + a^2)$. It follows that the gain reduction $G/G_0 = (1 + a^2)^{-1}$ which for small a^2 becomes $-4{\cdot}34a^2$ dB, i.e. $G/G_0 \simeq -m^2$ dB; for example, with $m = 50\%$, $G/G_0 = -0{\cdot}26$ dB.

An interesting extension of this method is provided by restricting the odd component of the current distribution to the central two-thirds of the aperture so that we have

$$p_n(s) = -\mathrm{j}\frac{2aN}{3}\sin(\pi Ns/3)\ \mathrm{sinc}(\pi Ns/3)$$

by replacing N with $2N/3$ in Equation (6). This quadrature pattern equally fills the nulls at adjacent points $q = 1,\ 2;\ 4,\ 5;\ 7,\ 8;\ \ldots$ with $m_q = 3a/2$. In particular, the first two nulls have been filled and setting $m_1 = m_2 = 50\%$ requires $a = 1/3$ with a gain reduction $G/G_0 = -0{\cdot}32$ dB.

The advantage of using a co-phased null-filling pattern (derived from an odd amplitude distribution) in quadrature with the primary pattern is that the increase in pattern sidelobe levels above those of the unperturbed primary pattern is kept to a minimum. The fact that the null-filling is incomplete normally restricts the application of this method to v.h.f., where null-filling the first one or two pattern zeros is sufficient.

3.1.2. 'Twin-beam' Method

The principle of this pattern shaping method is that a smooth null-filled pattern can be obtained by the complex addition of two sinc patterns, one real and the other imaginary, that are also displaced relative to each other along the ψ axis by $\pi/2$; the pattern is proportional to $(1/\psi)\exp \mathrm{j}\psi$ for large ψ and has a cosecant envelope $1/\psi$. The resulting distribution turns out to be co-phased over the aperture, with an amplitude variation corresponding to a quarter-sine-wave.

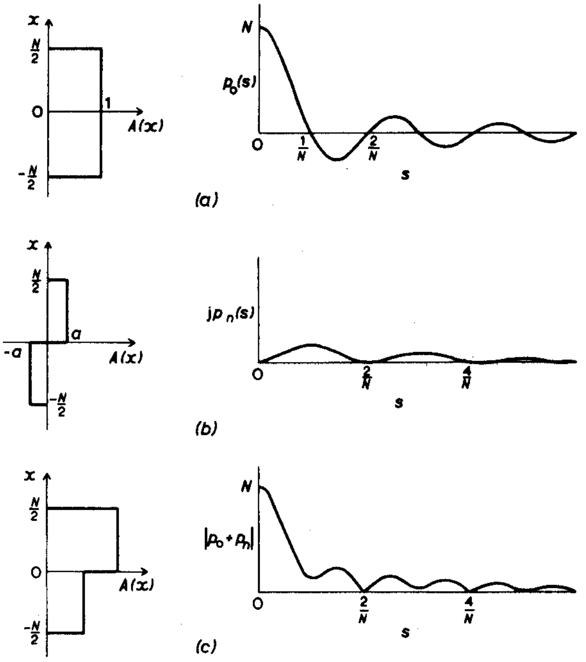

Fig. 2 - Null-filling by unequal power division

(*a*) Even distribution and primary pattern p_0
(*b*) Odd distribution and quadrature pattern p_n
(*c*) Net distribution and v.r.p. $|p_0 + p_n|$

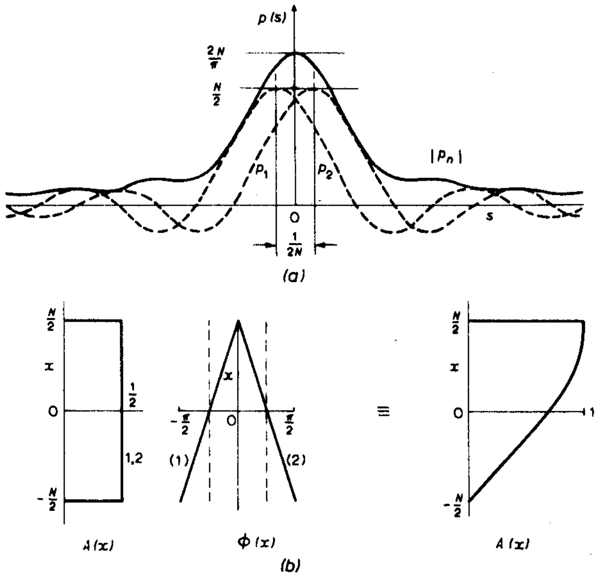

Fig. 3 - The principles of the twin-beam method

(*a*) Pattern components and net v.r.p.
(*b*) Amplitude and phase distributions

The process is illustrated in Fig. 3 for an $N\lambda$ aperture. The first half-pattern (or 'beam') is a sinc function phase-retarded by $\pi/4$ and beam-tilted along the s axis by $1/4N$ (downwards); the second half-pattern is also a sinc function phase-advanced by $\pi/4$ and beam-tilted along the s axis by $-1/4N$ (upwards), i.e.

$$p_1(s) = \frac{N}{2}\exp(-\mathrm{j}\pi/4)\ \mathrm{sinc}(Ns - 1/4)$$

$$p_2(s) = \frac{N}{2}\exp(\mathrm{j}\pi/4)\ \mathrm{sinc}(Ns + 1/4)$$

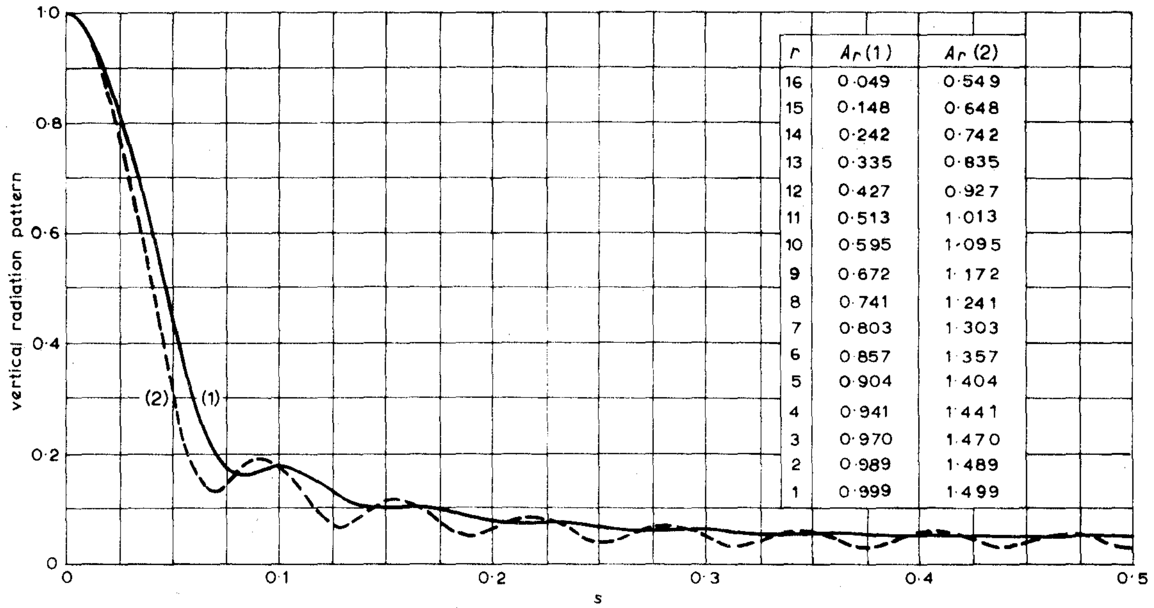

r	$A_r(1)$	$A_r(2)$
16	0·049	0·549
15	0·148	0·648
14	0·242	0·742
13	0·335	0·835
12	0·427	0·927
11	0·513	1·013
10	0·595	1·095
9	0·672	1·172
8	0·741	1·241
7	0·803	1·303
6	0·857	1·357
5	0·904	1·404
4	0·941	1·441
3	0·970	1·470
2	0·989	1·489
1	0·999	1·499

Fig. 4 - Computed v.r.p.s for a 16λ array of isotropic sources: null-filling by the twin-beam method at intended levels m = 1·0, 0·5

(1) ———— $b = 0$ (2) – – – – – $b = 0{\cdot}5$

The net radiation pattern is given by the complex sum of p_1 and p_2; provided that $Ns >> 1/4$ the denominators in both sinc functions can be approximated by πNs so that we have,

$$p_n(s) = p_1(s) + p_2(s)$$

$$\simeq \mathrm{j}\,\frac{\exp(-\mathrm{j}\pi Ns)}{2\pi s} \qquad (7)$$

which is the required 100% null-filled pattern. The corresponding component distributions are uniform in amplitude and similarly phased by $\mp\pi/4$ together with phase progressions of $\pm\pi/2.\lambda$rad/wavelength respectively to allow for the beam-tilts. The net current distribution $I(x)$ is given by the sum of the two components which gives $\phi(x) = 0$ and,

$$A(x) = \cos\frac{\pi}{2}(x/N - 1/2)$$

$$[-N/2 \leqslant x \leqslant N/2] \qquad (8)$$

which is a 'quarter-sine' amplitude distribution. Inverting the distribution of Equation (8) simply reverses the phase of the complex radiation pattern (Equation (7)).

It is possible to reduce the degree of null-filling to any desired level by adding a uniform 'pedestal' amplitude distribution to the quarter-sine distribution. The patterns from both distributions have cosecant envelopes and their sidelobes are co-phased at the peaks (c.f. Equations (5) and (7)). It follows that, if the height of the pedestal distribution is b so that $I(x) = A(x) + b$, the resultant null-filling becomes

$$m = 1/(1 + 2b) \qquad (9)$$

and is uniform throughout. It can be shown that the gain reduction due to null-filling is given by the expression $G/G_0 = \{(2/\pi) + b\}^2/\{½ + (4b/\pi) + b^2\}$. Fig. 4 shows null-filled v.r.p.s* for a 16 source array; the current distributions have been derived from the equivalent aperture with $N = 16$, $b = 0$ and $b = 1/2$, by sampling $I(x)$ at 1·0λ intervals ($x = 0{\cdot}5$, $1{\cdot}5, \ldots 15{\cdot}5$). The computed v.r.p.s show good approximations to smooth null-fillings of $m = 1{\cdot}0$ and $m = 0{\cdot}50$ as predicted by Equation (9); the respective gain losses are 0·91 dB (curve 1) and 0·31 dB (curve 2)

Although the method is seen to provide smooth null-filling, the main disadvantage is that, for a reasonable degree of fill, excessive amplitude variation leads to a few tiers of the aerial carrying a disproportionate amount of power. For example, in the above case for $N = 16$ and $m = 75\%$ ($b = 1/6$) the uppermost tier carries 84% more power than it would do if the aerial were uniformly fed; moreover, the upper two tiers together carry almost a quarter of the total power. Another drawback with the method is the uncontrollable null-filling above the horizontal which results in twice as much gain reduction as is necessary.

---

* Computed v.r.p.s are normalized to unity, i.e. the amplitude of the main beam $\hat{p}(s) = 1$.

3.2. Constant-Amplitude Solutions

Constant-amplitude current distributions lead to uniform power division over the aerial aperture and the required phase variations are realized easily by adjusting the lengths of the branch-feeders to the individual aerial tiers.

3.2.1. Phase Perturbation

The principles of this null-filling method have been described elsewhere[10] and a detailed account given in a previous BBC Research Department Report[11]. Here it will be sufficient to outline the main techniques.

Commencing with an unperturbed uniform aperture having a real sinc pattern p_0, null-filling is obtained by adding to it a suitably shaped imaginary secondary pattern p_n; i.e. the null-filled pattern is given by $p_0 + \mathrm{j}p_n$. The imaginary or quadrature pattern p_n is made even, so that the corresponding even current distribution I_n is also co-phased, but in quadrature with the uniform primary distribution. In order to make the resultant distribution $I(x)$ of constant unit amplitude, the primary distribution is adjusted from unity to $(1 - |I_n|^2)^{1/2}$ over the aperture. The quadrature pattern p_n is built up from elementary sinc patterns whose main beams are positioned at the primary null-points so that the null-filling levels and polarity can be varied over the pattern.

The synthesis process for the so-called 'oscillatory' solution is shown in Fig. 5. Elementary quadrature sinc patterns satisfy the cosecant requirements with amplitudes $m_q N/\pi q$ and oscillate in polarity at successive null-points, $q = \pm 1, \pm 2, \pm 3 \ldots$; the nulls above the horizontal (q negative) are filled because the null-filling distribution is co-phased. The beam-tilt associated with the qth pair of sinc patterns is $\pm q/N$; it follows that the corresponding elementary quadrature current distributions have constant amplitude $m_q/\pi q$ and equal and opposite phase progressions $\exp(\pm \mathrm{j}2\pi qx/N)$. Each pair of sinc patterns therefore corresponds to a current distribution $\mathrm{j}(2m_q/\pi q)\cos(2\pi qx/N)$ and the net distribution for all pairs in combination is given by

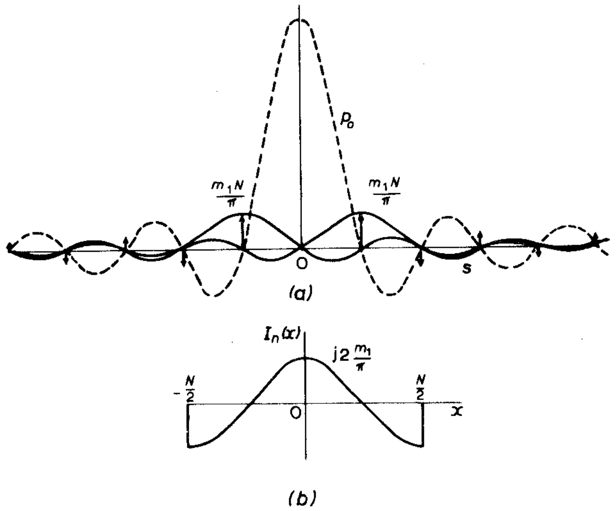

Fig. 5 - Null-filling by phase perturbation: oscillatory solution

(*a*) Elementary pair of null-filling patterns
(*b*) Corresponding quadrature distribution

$$I_n(x) = \pm \mathrm{j} \sum_{q=1}^{N/2} (-1)^q \left(\frac{2m_q}{\pi q}\right) \cos\left(\frac{2\pi qx}{N}\right) \qquad (10)$$

Equation (10) is an expression for the continuous quadrature current distribution which is to be simulated by a point-source array. For the rth pair of sources, located at $x = \pm(2r - 1)/2$, Equation (10) gives an explicit formula for their phase perturbation $\phi_r \simeq \sin \phi_r$

$$= |I_n(x)|,$$

$$\phi_r \simeq \sin \phi_r$$

$$= \pm \sum_{q=1}^{N/2} (-1)^q \left(\frac{2m_q}{\pi q}\right) \cos\left\{\frac{(2r-1)\,\pi q}{N}\right\} \qquad (11)$$

The complete constant amplitude current distribution for the array is $\cos \phi_r \pm \mathrm{j} \sin \phi_r$ where $\cos \phi_r$ is the modified primary distribution and the entire quadrature distribution can be leading or lagging.

An important feature of the oscillatory solution is that the null-filling pattern p_n is made to cross the s axis near to the points at which the primary pattern reaches its sidelobe maxima; this means that the sidelobes of the null-filled v.r.p. will have amplitudes which are little different from those of the primary pattern. Although there is no null-filling at $s = \pm 1/2$, (30°), because ϕ_r is even, it can be introduced if required by adding a small oscillatory and odd phase perturbation on to ϕ_r[11].

In the alternative 'non-oscillatory' solution, elementary sinc patterns are again made to follow the specified cosecant envelope but are of identical polarity. The phase perturbations are given by the summation of Equation (11) by making the coefficients of the cosine terms all positive (or negative). The result is the exact inversion of that given by the previous solution, i.e. $\phi_r = \phi^{(osc)}_{N/2+1-r}$ and vice versa. With this solution, however, the sidelobe levels in the net v.r.p. are greatly distorted from the cosecant envelope and this has to be corrected. Correction is effected by adding an odd differential phase shift 2Δrad on to ϕ_r (i.e. $+\Delta$ for the upper half, $r>0$ and $-\Delta$ for the lower half $r<0$). A semi-empirical relation for Δ which works

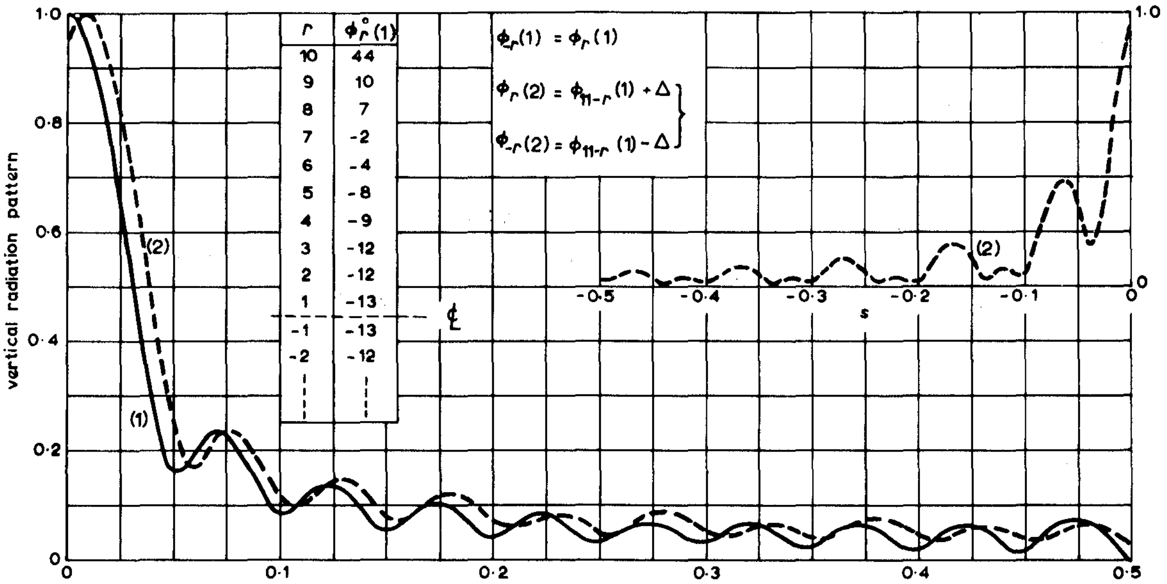

Fig. 6 - Computed v.r.p.s for a 20λ array of isotropic sources: null-filling by phase perturbation with m = 0·5
(1) ———— oscillatory solution (2) – – – – – non-oscillatory solution ($\Delta = 20^\circ$)

reasonably well in practice is

$$\Delta \simeq \tfrac{1}{2}\phi_1^2 \sin (5\pi/N) \qquad (12)$$

where ϕ_1 is the relative phase of the innermost pair of sources i.e. $\phi_{N/2} = 0$. A secondary effect of differential phase correction is that it produces an incidental beam-tilt of approximately $2\Delta/\pi N$ which must be allowed for when choosing the phase progression for final beam-tilt.

The gain reduction G/G_0 of a phase-perturbed array is approximately $-4{\cdot}34\sigma_\phi^2$ dB where σ_ϕ is the standard deviation of ϕ_r; this result is in very good agreement with the figures obtained from pattern integration. Since for uniform null-filling (m_q constant), ϕ_r is proportional to m (Equation (11)), G/G_0 is proportional to m^2. For example, with a 20λ array, $m = 0{\cdot}50$ gives $G/G_0 = -0{\cdot}4$ dB and $m = 0{\cdot}25$ gives $G/G_0 = -0{\cdot}1$ dB.

Computed v.r.p.s for a 20λ array with null-filling obtained from the two solutions are shown in Fig. 6; the intended null-filling was 50%. The beam-tilt with the non-oscillatory solution (curve 2) has not been re-adjusted to zero. Computed gain losses are 0·35 dB (curve 1) and 0·49 dB (curve 2). The behaviour of the patterns is typical and both solutions are satisfactory in respect of null-filling.

It must be noted that null-filling obtainable from the phase-perturbation method is limited to about 60% ($m \simeq 0{\cdot}6$) since above this figure the approximations involved break down. Although the method offers the advantage that null-filling can be individually adjusted at each null-point, it is not possible to control the pattern shape above the horizontal.

3.2.2. Stationary-Phase Method

A detailed account of this pattern-shaping technique and its application to null-filling has been given in a previous BBC Research Department Report[12]. The method is based on a 'stationary-phase' solution of the radiation-pattern integral and involves the type of approximation used in geometrical-optics; it is therefore restricted to aerials whose apertures are large compared with the wavelength. The necessary results are derived here using heuristic arguments.

We consider a linear source of constant amplitude with current distribution $\exp\{j\phi(x)\}$ along its length $N\lambda$ with x referred to the base of the source (Fig. 7(*a*) and (*b*)). The complex pattern is given by the following pattern integral,

$$p(s) = \frac{1}{k}\int_0^N \exp j\{\phi(x) - 2\pi xs\}\, dx$$

where k is the pattern magnitude; the significance of k will appear later. Suppose now that $x = \alpha$ is a point of *stationary phase* for a particular declination s, i.e. at $x = \alpha$ we have,

$$\phi'(x) = 2\pi s \qquad (13)$$

where $\phi'(x)$ denotes the first derivative of $\phi(x)$ with respect to x at $x = \alpha$. For large N, the integrand of the pattern integral will be highly oscillatory except near $x = \alpha$, where the phase is stationary*, so that the major contribution to the integral comes from an incremental aperture length δx in the immediate vicinity of the stationary point; the declination corresponding to this point is given by Equation (13). It is now assumed that each increment of aperture δx is a radiating source which directs practically all its energy over a narrow angular range δs which is centred on the stationary-phase declination. This assumption is consistent with the fact that the total real powers in the aperture and the radiation pattern must be identical. Since $A(x) = 1$ throughout, equating the incremental powers at $x = \alpha$ we obtain,

---

* The point $x = \alpha$ is assumed to be single-valued.

$$k^2 |p(s)|^2 \delta s \simeq \delta x$$

But from Equation (13) we also have the relation,

$$\phi''(x) \delta x \simeq 2\pi \delta s$$

where $\phi''(x)$ is the second derivation of $\phi(x)$ with respect to x at $x = \alpha$. Combining these two relations gives the result,

$$k^2 |p(s)|^2 \phi''(x) \simeq 2\pi \tag{14}$$

Equations (13) and (14) are the basis of pattern synthesis by the stationary-phase method for constant amplitude distributions. Together they form a non-linear second order differential equation which must be solved in order to determine the phase distribution $\phi(x)$ required to give a particular power pattern $|p(s)|^2$.

For a cosecant pattern we put $|p(s)| = 1/s$ in Equation (14). Energy considerations limit the synthesis to a finite angular range, i.e. $s_1 \leqslant s \leqslant s_2$ (Fig. 7(*c*)), and the pattern magnitude k is directly determined by the limits s_1 and s_2 together with the constants of integration. Finally, the solution of the differential equation gives

$$\phi(x) \simeq -2\pi k^2 \log(1 - s_1 x / k^2) \tag{15}$$

with

$$k^2 = N / (s_1^{-1} - s_2^{-1}) \tag{16}$$

where the phase-reference point for the source is taken at the base of the aperture, i.e. $\phi(0) = 0$. The phase-slope of the distribution $\phi'(x)$ at the point which radiates in direction s is $2\pi s$ rad/wavelength so that the largest slope occurs at the top of the aperture ($x = N$, $s = s_2$). If the inverted phase distribution $-\phi(N - x)$ is employed instead, the largest slope is at the base of the aperture ($x = 0$, $s = s_2$).

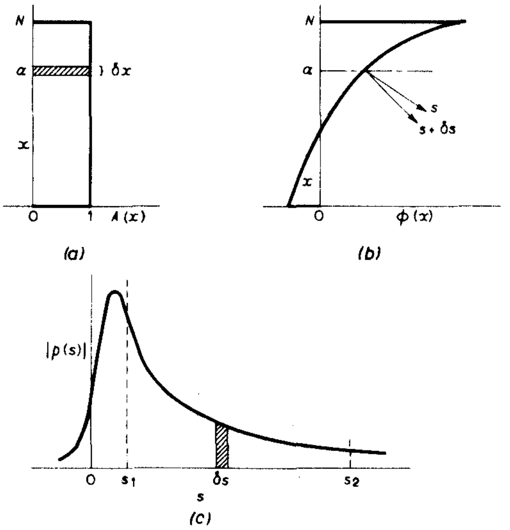

Fig. 7 - The stationary-phase method: Nλ aperture with current distribution $\exp\{j\phi(x)\}$

(*a*) Constant amplitude distribution
(*b*) Phase distribution $\phi(x)$
(*c*) Radiation pattern $|p(s)|$

Computed v.r.p.s for a 16λ array with phase distributions given by Equations (15) and (16) for a small range of k are shown in Fig. 8; the gain reductions are respectively 0·54 dB (curve 1), 1·00 dB (curve 2) and 1·85 dB (curve 3). Since the main beam of the pattern is partially included in the approximation to the cosecant shape, null-filling is not uniform (m_q varies with q) and, equally important, some incidental beam-tilt is introduced. The overall degree of null-filling can be adjusted by varying s_1 which also changes the beam-tilt, as shown in Fig. 8. The pattern shape is relatively insensitive to changes in s_2. Since m_q is nearly proportional to k over a large range of q, in those cases where $s_2 \gg s_1$ we have m_q proportional to $s_1^{1/2}$. Null-filling adjustment would normally be carried out at the most important null-point, i.e. at the first null ($q = 1$).

The method is easily extended to cases where there exists non-uniform power division over the aperture by matching the phases, phase gradients and patterns at the crossover points (Section 3.3.4.).

There is no limitation in null-filling level with the stationary-phase method although the pattern minima obtained can be quite non-uniform; in addition, sidelobe levels become rather high for large degrees of filling. The main advantage of the method is that there is no intentional null-filling above the horizontal; a disadvantage is the resulting oscillatory pattern and the rather high gain reduction.

3.3. Variable Amplitude-and-Phase Solutions

Admitting variable amplitudes and phases in the current distribution of an array allows the full number of degrees of freedom ($2N - 1$) to be utilized in pattern shaping so that the synthesis accuracy and flexibility are greatly increased. Some of the techniques to be discussed are 'hybrid' solutions of previously described methods.

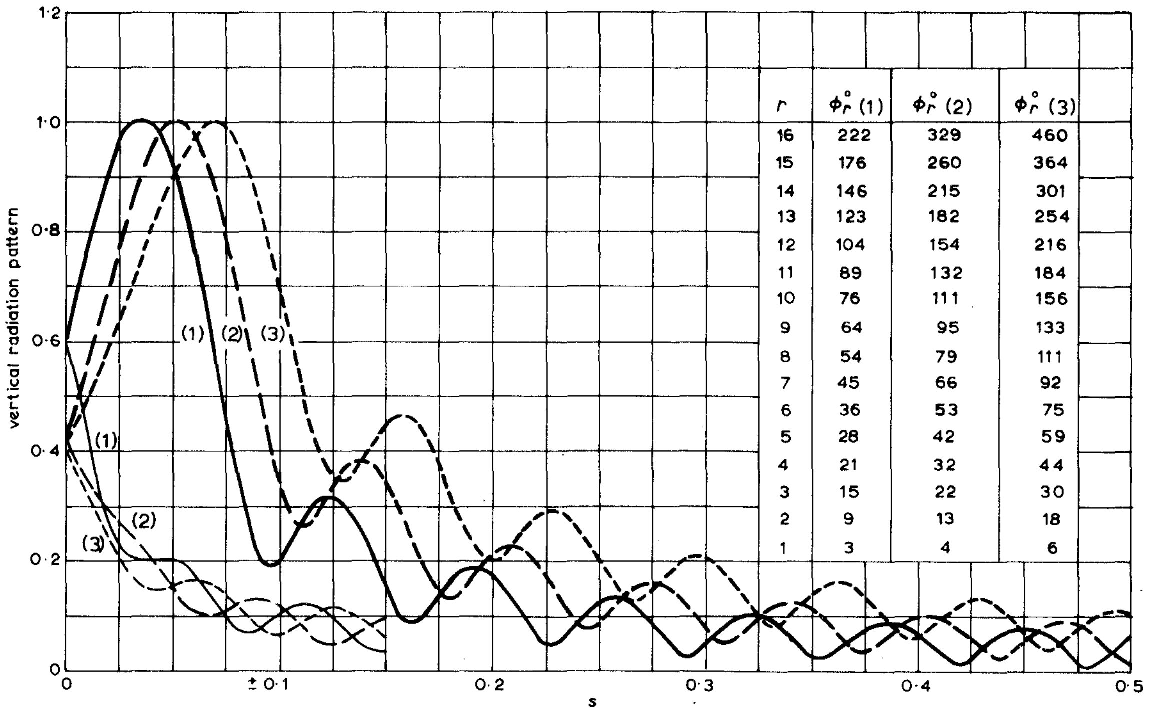

r	ϕ_r° (1)	ϕ_r° (2)	ϕ_r° (3)
16	222	329	460
15	176	260	364
14	146	215	301
13	123	182	254
12	104	154	216
11	89	132	184
10	76	111	156
9	64	95	133
8	54	79	111
7	45	66	92
6	36	53	75
5	28	42	59
4	21	32	44
3	15	22	30
2	9	13	18
1	3	4	6

Fig. 8 - Computed v.r.p.s for a 16λ array of isotropic sources: null-filling by the stationary-phase method with $s_2 = 0{\cdot}5$ *and* $k = k(s_1)$ *as parameter*

(1) ——— $k = 0{\cdot}508$, $s_1 = 0{\cdot}0156$ (2) — — — $k = 0{\cdot}617$, $s_1 = 0{\cdot}0227$ (3) - - - - - $k = 0{\cdot}730$, $s_1 = 0{\cdot}0312$

3.3.1. Central-Tiers Method

In this method a tier or group of tiers located at the centre of an otherwise uniform aerial is fed with additional current of chosen amplitude and phase in order to provide null-filling[13]. The null-filling is generally crude and limited to a small range of declinations.

In the simplest method, a single source at the centre of the aerial is fed with quadrature current. This gives null-filling with m_q increasing with q, although the rise in m_q can be reduced to some extent by making the source vertically directional.

As an example of this technique, suppose that additional current is limited to a central section, width $M\lambda$ of an $N\lambda$ aperture and is in phase quadrature with the primary current. The primary pattern p_0 is N sinc(Ns) and if the secondary current over the central $M\lambda$ is constant and of amplitude c the null-filling pattern p_n is cM sinc(Ms). It follows that the degree of null-filling obtained is given by

$$m_q \simeq c\ \sin(\pi q M/N) \qquad (17)$$

Equation (17) shows that the null-filling is oscillatory over the pattern and will disappear at periodic nulls if N/M is integral. For example, if $c = 1/\sqrt{3}$ and $N/M = 3$, $m_q = 0{\cdot}50$ for $q = 1, 2, 4, 5, \ldots$ and $m_q = 0$ for $q = 3, 6, 9, \ldots$ (c.f. Section 3.1.1.); the gain reduction is approximately 0·25 dB. Alternatively, if the pattern p_n is beam-tilted by $1/N$ by progressively phasing the secondary current across the central section, we can select m_1 by making $c = m_1 N/\pi M$; now if $N/M = 3$ and m_1 is set to 0·50 we obtain $m_2 \simeq 0{\cdot}85$, $m_3 \simeq 0{\cdot}63$ and $m_4 = 0$ and so on. Phasing the currents in the central tiers has increased the number of filled nulls. Obviously more complicated solutions are possible especially if amplitude variation is also introduced to shape the null-filling pattern due to the central tier(s).

The method, though simple, provides limited null-filling which is not easily controllable; it would be useful if null-filling were required over only a small range of declinations e.g. at v.h.f.

3.3.2. Woodward's Cosecant Solution

In this pattern-shaping technique, a real (co-phased) cosecant pattern is synthesized from an $N\lambda$ aperture by directly superimposing elementary co-phased sinc patterns; the main beams of these pattern components are positioned every $1/N$ on the s axis and their magnitudes are determined by the corresponding cosecant amplitudes which are required at each declination. An example, taken from Woodward's classic paper[14], is shown in Fig. 9 for the case of a 10λ aperture. The vertical lines on the pattern (Fig. 9(a)) represent the magnitudes of the elementary beams referred to the beam at $s = 1/N$ (one such beam has been drawn in). A maximum of $2N + 1$ (i.e. 21) magnitudes may be

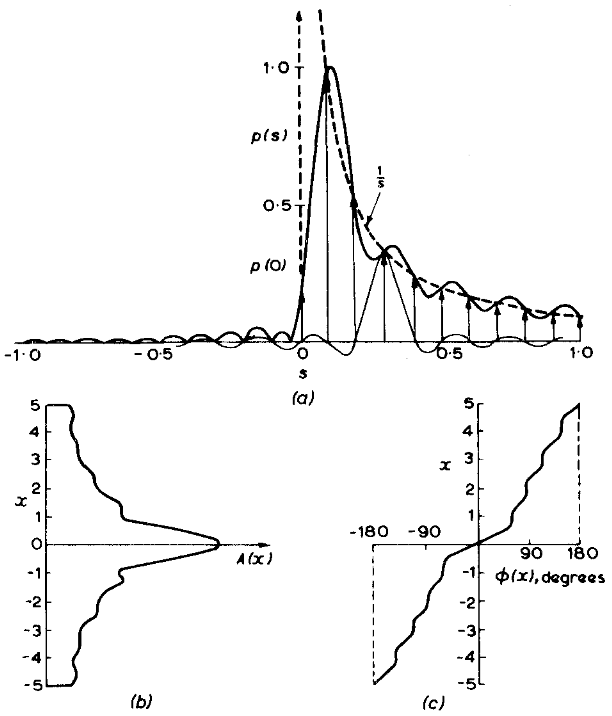

Fig. 9 - Synthesis of a cosecant radiation pattern by Woodward's method, N = 10 (taken from Reference 14)
(a) Radiation pattern (b) Amplitude distribution
(c) Phase distribution

specified and, in the example shown, eleven have been made non-zero. The choice of $p(0)$ is arbitrary since the pattern is indeterminate at $s = 0$. Woodward has shown, however, that the sidelobe level above the horizontal is a minimum for $p(0) \simeq 0{\cdot}6$. The best approximation to a cosecant pattern below the horizontal occurs when $p(0)$ is approximately equal to 0·8 but the amplitude distribution then varies considerably over the aperture.

The aperture distribution is even in amplitude and odd in phase because the synthesized pattern is co-phased. The complex current distribution $I(x)$ is obtained from the summation

$$I(x) = \sum_{q=0} p(q/N) \exp(\mathrm{j}2\pi qx/N) \qquad (18)$$

where $p(q/N)$ are the specified pattern amplitudes and the exponential terms are the linear progressive phase shifts required for beam-tilting the corresponding elementary sinc patterns. For a cosecant pattern, $p(q/N)$ are set to $p(0)$, 1·0, 0·50, 0·333, . . . etc. with $p(0)$ arbitrary; the value of $p(0)$ will determine the effective degree of null-filling and also the inherent beam-tilt in the resultant pattern.

Fig. 10 shows computed v.r.p.s for a 16λ array of isotropic sources with cosecant weighted beams placed at s = 0, 1/16, 1/8, . . . 1/2 following Woodward's original scheme; in curve (1), $p(0) = 0{\cdot}50$ and in curve (2), $p(0) = 0$. Both patterns are good approximations to the desired cosecant shape (broken curve) with the main lobes partially contributing to the approximations; they differ only in their $p(0)$ beams i.e. the difference between curves (1) and (2) is approximately ½sinc(10s). The equivalent null-filling, however, is excessive. Sidelobe widths have almost doubled in the process and the gain reduction is large (2·45 dB (curve 1) and 1·59 dB (curve 2) respectively); moreover, the amplitude variation in the current distribution is very high.

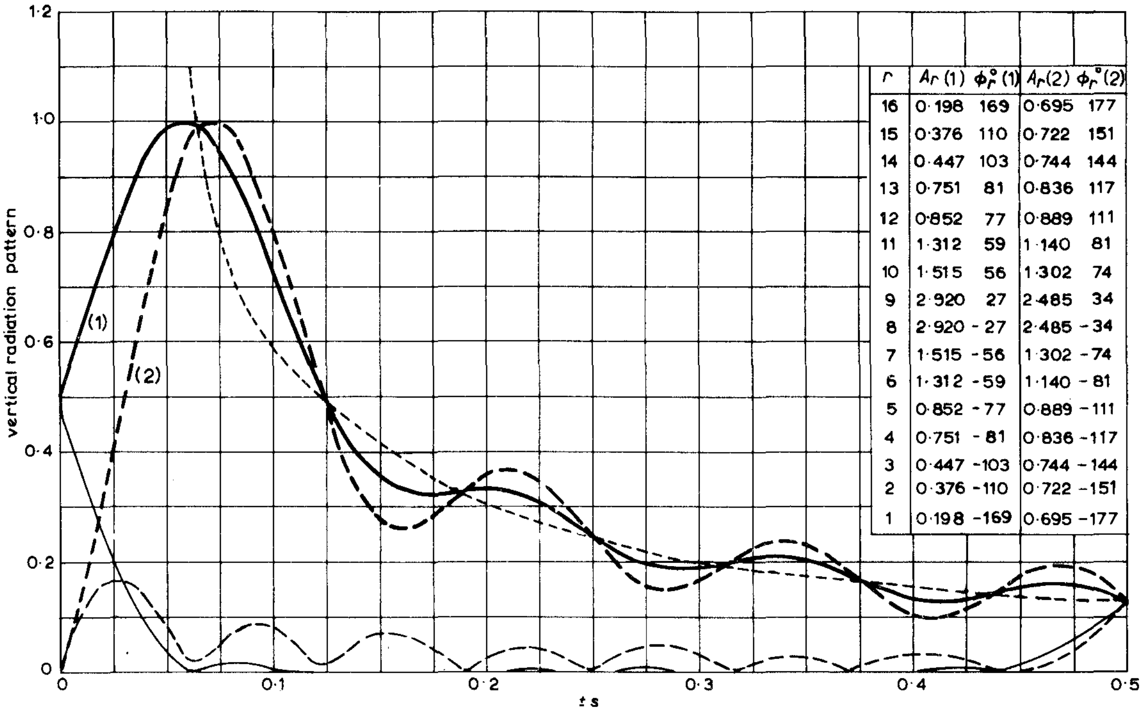

r	$A_r(1)$	$\phi_r^\circ(1)$	$A_r(2)$	$\phi_r^\circ(2)$
16	0·198	169	0·695	177
15	0·376	110	0·722	151
14	0·447	103	0·744	144
13	0·751	81	0·836	117
12	0·852	77	0·889	111
11	1·312	59	1·140	81
10	1·515	56	1·302	74
9	2·920	27	2·485	34
8	2·920	-27	2·485	-34
7	1·515	-56	1·302	-74
6	1·312	-59	1·140	-81
5	0·852	-77	0·889	-111
4	0·751	-81	0·836	-117
3	0·447	-103	0·744	-144
2	0·376	-110	0·722	-151
1	0·198	-169	0·695	-177

Fig. 10 - Computed v.r.p.s for a 16λ array of isotropic sources: null-filling by the 'Woodward-cosecant' method
(1) ———— $p(0) = 0{\cdot}50$ (2) — — — — $p(0) = 0$ - - - - - - - - cosecant envelope

It would appear that, although the method works very well for cosecant pattern synthesis, its direct application to null-filling is limited by the difficulty of finding a satisfactory set of amplitudes for the synthesizing beams in order to control the pattern minima to an acceptable level. In addition, the large current variation and high gain reduction and beamwidth would normally be unacceptable. The method, however, has been used for single-channel u.h.f. aerials[15].

3.3.3. Current Perturbation ('Woodward-Quadrature')

This null-filling method employs a synthesis technique which is similar to that employed in the oscillatory phase perturbation solution (Section 3.2.1.); the essential difference is that, in the present method, the current distribution is not re-adjusted to be constant amplitude after null-filling synthesis so that the quadrature null-filling pattern can be restricted to positive declinations; the latter pattern is synthesized by the Woodward method. The oscillatory solution is normally used in order to minimize sidelobe perturbation in the resultant pattern and this leads to smooth null-filled patterns.

The starting point for synthesis is again the pattern of a uniform co-phased aperture N sinc(Ns); this is the primary pattern p_0 (Fig. 5(a)). The nulls in this pattern which appear at $s = q/N$ are filled by elementary sinc patterns placed everywhere in phase quadrature with p_0. The amplitudes of the secondary beams $m_q N/\pi q$ are determined by the required degree of null-filling m_q at each null-point and they are made to oscillate in polarity over successive nulls. The beam-tilt associated with the qth sinc pattern is q/N so that the corresponding elementary current distribution is

$$\pm \mathrm{j}(-1)^q (m_q/\pi q)\exp(\mathrm{j}2\pi q x/N)$$

over the aperture. The summation of all such distributions leads to the net secondary current distribution* $I_n(x)$ and superposing this on to the primary distribution gives the following expression for the resultant current distribution,

$$I(x) = 1 \pm \mathrm{j}\sum_{q=1}(-1)^q\left(\frac{m_q}{\pi q}\right)\exp\left(\mathrm{j}\frac{2\pi q x}{N}\right) \qquad (19)$$

Equation (19) gives the continuous complex current distribution which is to be sampled at points $x = -N + 0{\cdot}5, -N + 1{\cdot}5, \ldots, -0{\cdot}5, 0{\cdot}5, \ldots N - 0{\cdot}5$, in order to give the source currents for an $N\lambda$ array to synthesize a null-filled v.r.p. with specified levels m_q. There is no even or odd symmetry in the resultant amplitude and phase distributions in $I(x)$; the v.r.p. will exhibit a small inherent beam-tilt.

Examples of non-uniform null-filling are given in Fig. 11 which shows computed v.r.p.s for a 16λ array of isotropic sources. In the first example (curve 1) the intended null-filling was $m_q = 0{\cdot}70$ for $q = 1, 2, 3, 4$ and $m_q = 0{\cdot}50$ for $q = 5, 6, 7, 8$; in the second example (curve 2) the intended null-filling was $m_q = 0{\cdot}50$ and $m_q = 0$ over the same ranges respectively. Synthesis is seen to be reasonably accurate and the gain reductions (0·35 dB (curve 1) and 0·15 dB (curve 2) respectively) are not excessive; moreover, even with a large degree of null-filling, variations in the amplitude distribution of source currents are not unduly high.

The method is easy to apply and offers the advantage of providing accurate null-filling where required; in particular the pattern is not null-filled above the horizontal although the primary component remains at full amplitude.

3.3.4. General Stationary-Phase Methods

The stationary-phase method of pattern shaping (Section 3.2.2) is not restricted to apertures of constant amplitude since the radiation-pattern integral can also be approximately solved in cases where varying amplitude functions $A(x)$ weight the exponential phase term. The synthesis equation is Equation (14) with the right hand side replaced by $2\pi A^2(x)$. By choosing a phase distribution which satisfies the conditions of stationary phase, amplitude distributions can be found[4] which provide reasonable approximations to cosecant patterns. However, for practical reasons we are normally interested in deriving phase distributions which give cosecant-shaped patterns from those amplitude distributions which can be easily realized practically.

We have already shown that the co-phased quarter-sine-wave distribution gives good approximations to smooth 100% null-filled patterns (Section 3.1.2). In practice, however, the large amplitude variation (and hence also the null-filling) can be reduced by adding a pedestal distribution. Starting from such a distribution the stationary-phase method can be used to derive a phase distribution which re-adjusts the null-filling and incidentally improves the pattern by removing the symmetry and reducing radiation above the horizontal. For practical reasons the actual distribution is normally approximated by a stepped amplitude profile.

The basis of the stepped-amplitude stationary-phase solution is best demonstrated by synthesizing a cosecant pattern from a simple one-step amplitude distribution. Fig. 12(a) shows an $N\lambda$ aperture with non-uniform power division over its length. The aperture is divided into two unequal sections of constant amplitude with $A(x) = A_1$ for $0<x<M$ and $A(x) = A_2$ for $M<x<N$. The lower section is used to synthesize the pattern over the range $s_1 \leqslant s < s_{12}$ and the upper section over the range $s_{12} < s \leqslant s_2$ where

---

* $I_n(x)$ is even in amplitude and odd in phase because the elementary null-filling sinc patterns are mutually co-phased.

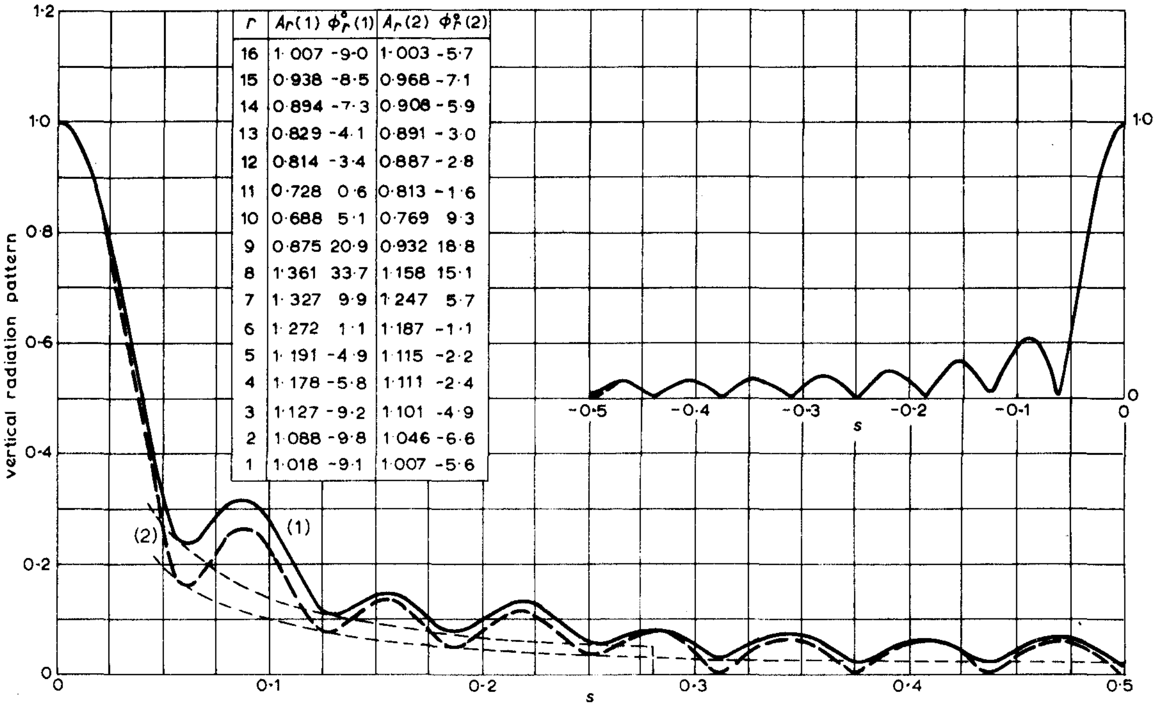

r	$A_r(1)$	$\phi^\circ_r(1)$	$A_r(2)$	$\phi^\circ_r(2)$
16	1·007	-9·0	1·003	-5·7
15	0·938	-8·5	0·968	-7·1
14	0·894	-7·3	0·908	-5·9
13	0·829	-4·1	0·891	-3·0
12	0·814	-3·4	0·887	-2·8
11	0·728	0·6	0·813	-1·6
10	0·688	5·1	0·769	9·3
9	0·875	20·9	0·932	18·8
8	1·361	33·7	1·158	15·1
7	1·327	9·9	1·247	5·7
6	1·272	1·1	1·187	-1·1
5	1·191	-4·9	1·115	-2·2
4	1·178	-5·8	1·111	-2·4
3	1·127	-9·2	1·101	-4·9
2	1·088	-9·8	1·046	-6·6
1	1·018	-9·1	1·007	-5·6

Fig. 11 - Computed v.r.p.s for a 16λ array of isotropic sources: null-filling by current perturbation ('Woodward-quadrature')

(1) ———— $m_q = 0{\cdot}70 (q = 1,2,3,4)$; $m_q = 0{\cdot}50 (q = 5,6,7,8)$ (2) — — — — $m_q = 0{\cdot}50 (q = 1,2,3,4)$

- - - - - - - null-filling references, $m = 70\%/50\%$

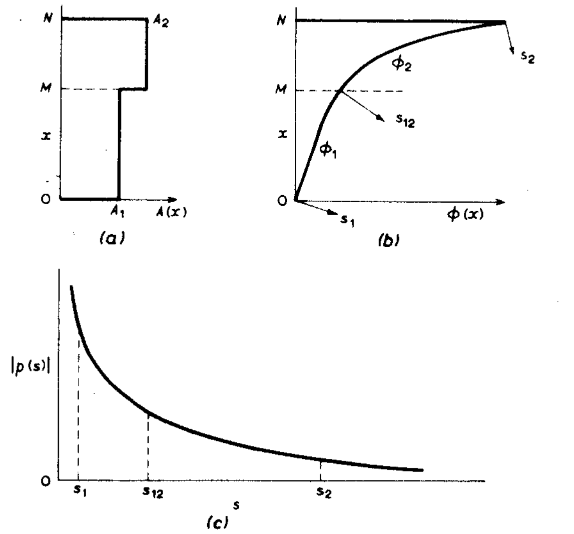

Fig. 12 - Stationary-phase method extended to stepped amplitude distributions

(a) Amplitude distribution
(b) Phase distributions ϕ_1, ϕ_2 (c) Radiation pattern

s_{12} has to be determined (Fig. 12(*c*)). The analysis is greatly simplified if the total radiated power is set equal to that radiated by the same aperture uniformly fed with $A(x) = 1$; we then have

$$MA_1^2 + (N - M)A_2^2 = N.$$

The magnitude of the power pattern k^2 is then given by Equation (16) as before and it can be shown that the declination s_{12} at which the patterns due to the two sections meet is given by,

$$s_{12} = Ns_1s_2/\left\{MA_1^2s_1 + (N - M)A_2^2s_2\right\} \qquad (20)$$

provided that the phase distribution $\phi(x)$ is made continuous* at $x = M$. Phase distributions $\phi_1(x)$ and $\phi_2(x)$ over the lower and upper sections of the aperture can now be written directly, from Equation (15) as,

$$\phi_1(x) \simeq -\frac{2\pi k^2}{A_1^2} \log(1 - A_1^2 s_1 x/k^2) \qquad [0<x<M] \qquad (21)$$

and

$$\phi_2(x) \simeq \phi_1(M) - \frac{2\pi k^2}{A_2^2} \log\{1 - A_2^2 s_{12}(x - M)/k^2\} \qquad [M<x<N] \qquad (22)$$

For the uniformly fed aperture with $A_1 = A_2 = 1$ Equations (21) and (22) degenerate into Equation (15) by substituting Equations (16) and (20). This extension of the stationary-phase method has been used in cases where there are more than one step in the amplitude distribution. For a large number of steps, however, it is more convenient to obtain $\phi(x)$ directly from the synthesis equation (Equation (14)) by inserting $A(x) = \cos(\pi x/2N) + b$ (quarter-sine-wave plus pedestal).

---

* The phase-slope $\phi'(x)$ ($= 2\pi s$) is also continuous because the pattern is continuous over s_{12}.

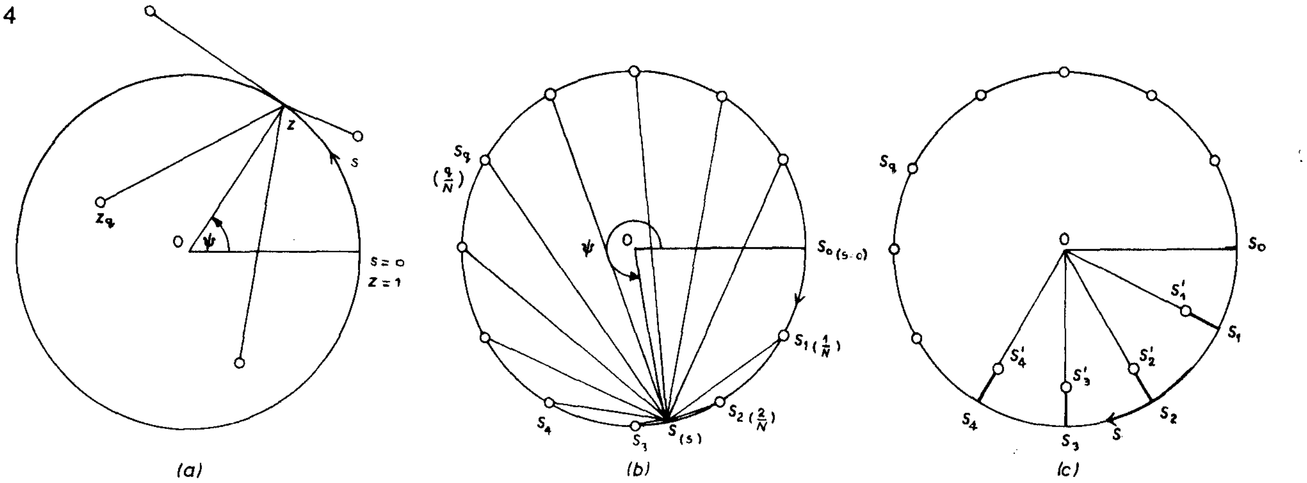

Fig. 13 - Null-filling by polynomial-zero perturbation

(a) z-plane diagram for equispaced array (b) z-plane diagram for uniform co-phased 12λ array
(c) radial perturbation of 4 polynomial zeros

The method suffers the same drawbacks as the constant-amplitude technique previously described but to a lesser extent, i.e. null-filling tends to be non-uniform and the pattern sidelobes become rather high. Nevertheless, quite acceptable results are produced; practical examples of this synthesis technique will be given in Section 4.2.2.

3.3.5. Polynomial-Root Perturbation

This null-filling method is based on the polynomial theory of linear arrays^6; it gives an accurate design in which the source-currents are directly determined by the levels of the pattern minima so that inaccuracies due to sampling a continuous distribution do not arise. Moreover, the pattern can be determined by simple calculation and, since the polynomial roots are known, the many other current distributions which provide the same power pattern are immediately available.

The complex radiation pattern of a linear array has been given previously by Equation (4). If the transformation $z = \exp(-j2\pi sd)$ is made in this equation, as in Reference 6, the pattern can be written as a polynomial in z i.e.

$$p(s) = f(z) = \sum_{r=0}^{N-1} I_r z^r = I_{N-1} \prod_{q=1}^{N-1} (z - z_q) \qquad (23)$$

The right hand side of Equation (23) is the factorial expression for the polynomial in which the z_q's are the zeros of $f(z)$ (Fig. 13(a)). As s increases, z describes a unit circle (anticlockwise) in the complex plane and $p(s)$ is the product of the vectors represented by lines joining z and the roots z_q; the amplitude of the pattern $|p(s)|$ is given by the product of the lengths of these vectors. If any of the roots z_q lie on the unit circle ($|z_q| = 1$) they correspond to nulls in the pattern $p(s)$ and occur at declinations s_q given by $\psi = \arg z_q = -2\pi s_q d$.

Now the pattern of a uniform co-phased array with $d = 1{\cdot}0\lambda$ is $\sin(N\pi s)/\sin(\pi s)$ and its nulls occur at $s_q = q/N$ so that the corresponding polynomial roots are equally spaced around the unit circle (Fig. 13(b)). The amplitude of the pattern $|p(s)|$ at any declination is given by the product $\overline{SS_1}\ \overline{SS_2}\ \overline{SS_3} \ldots \overline{SS_{N-1}}$. Suppose now that the zeros are moved radially inwards by small increments $\overline{S_1S'_1}$, $\overline{S_2S'_2}$, ... (Fig. 13(c)). There will be little error in taking $\overline{S_0S'_1} = \overline{S_0S_1}$, $\overline{S_0S'_2} = \overline{S_0S_2}$, etc. and assuming that the main beam of the pattern is still centred at $S_0(s = 0)$; it follows that $p(0) \simeq \overline{S_0S_1}\ \overline{S_0S_2}\ \overline{S_0S_3} \ldots\ldots \overline{S_0S_{N-1}}$ as before. Consider now, for example, the behaviour of $p(s)$ in the region of its second minimum, i.e. S near to S_2 (the second null-point). Obviously the position of this minimum must be very near to S_2 so that its amplitude is given quite accurately by the product $\overline{S_2S'_1}\ \overline{S_2S'_2}\ \overline{S_2S'_3} \ldots\ldots \overline{S_2S'_{N-1}}$ which is very close to $\overline{S_2S_1}\ \overline{S_2S'_2}\ \overline{S_2S_3} \ldots\ldots \overline{S_2S_{N-1}}$. But the original root locations s_q are uniformly spaced around the unit circle so that the amplitude of the second minimum can be re-written as the product $\overline{S_0S_1}\ \overline{S_2S'_2}\ \overline{S_0S_3} \ldots \overline{S_0S_{N-1}}$. If this amplitude is normalized to the amplitude of the main beam all the factors cancel except one and we are left with the quotient $\overline{S_2S'_2}/\overline{S_0S_2}$ for the normalized amplitude of the second pattern minimum; in null-filling terms this is identical to $m_2/\pi q$. For the qth minimum, therefore, we have the result,

$$\overline{S_qS'_q}/\overline{S_0S_q} \simeq m_q/\pi q$$

The chord length $\overline{S_0S_q}$ is $2\sin(\pi q/N)$ for a unit circle so that the final expression for the radial perturbation δR_q of the qth root required to give $100m_q$% null-filling at the qth pattern zero is

$$\delta R_q \simeq -\frac{2m_q}{\pi q}\sin(\pi q/N) \qquad (24)$$

The perturbed root locations are given by the vectors

$$z_q = (1 - \delta R_q)\exp(-j2\pi q/N) \qquad (25)$$

Equations (24) and (25) determine the polynomial factors $z - z_q$ which must be multiplied together to give the array polynomial $f(z)$. The coefficients of the terms z^r in $f(z)$ give the complex source currents I_r required for null-filling through Equation (23)*; unlike the pattern calculation, multiplication of the complex factors $z - z_q$ to determine the current distribution can be tedious for large N and it is recommended that this operation be performed by computer.

An example of the results which can be obtained by this technique is shown in Fig. 14; the first six nulls in the v.r.p. from a 16λ array have been filled at two intended levels (i.e. $m_1 = m_2 = m_3 = 0{\cdot}70$, and $m_4 = m_5 = m_6 = 0{\cdot}50$). Inspection of the computed pattern reveals a very high null-filling accuracy indeed. There is a very small incidental beam-tilt which has not been resolved by the computation (s interval 0·01); the v.r.p. has no unwanted null-filling and the gain reduction is only 0·32 dB.

Polynomial-root perturbation is the most accurate null-filling technique to be developed so far; null-fills can be individually specified and there are no errors due to sampling. With no unwanted null-filling above the horizontal, gain reduction is minimal.

3.4. Further Synthesis Solutions for Design Optimization

The synthesis methods described above give current distributions which provide different approximations to desired null-filled patterns. A particular solution can be optimum in that it leads to an acceptable v.r.p. and that the current distribution is of the required type but it may suffer the disadvantage that, for example, the amplitude distribution, or the aerial impedance, or the half-aerial v.r.p. is unacceptable. The polynomial theory outlined in Section 3.3.5 can lead to many other current distributions which provide identically shaped v.r.p.s. The exploration of further solutions by this approach is possible whatever the method used to obtain the first solution.

The method for determining all the distributions associated with a given null-filling design is derived as follows. The starting point is the polynomial expression $f(z)$ for the pattern $p(s)$ of a linear array (Equation (23)); the factorial expansion for pattern amplitude is given by,

$$|f(z)| = |z - z_1||z - z_2| \ . \ . \ . \ |z - z_q| \ . \ . \ . \ |z - z_{N-1}|$$

Suppose we select the qth root z_q and invert its amplitude R_q without changing its phase $\psi_q(=-2\pi s_q)$, i.e. replace z_q by its reciprocal complex conjugate $1/z_q^*$; this process is illustrated in Fig. 15. The factor $|z - z_q|$ now becomes $|z - 1/z_q^*|$ but since z is on the unit circle (i.e. $z = \exp \mathrm{j}\psi$) application of the cosine rule shows that,

$$|z - z_q| = R_q|z - 1/z_q^*|$$

In other words, inverting any non-unitary root of $f(z)$ will alter the magnitude of the pattern without changing its shape (i.e. variation with s). However,

---

* The current I_{N-1} may be regarded as a scaling factor and set to unity.

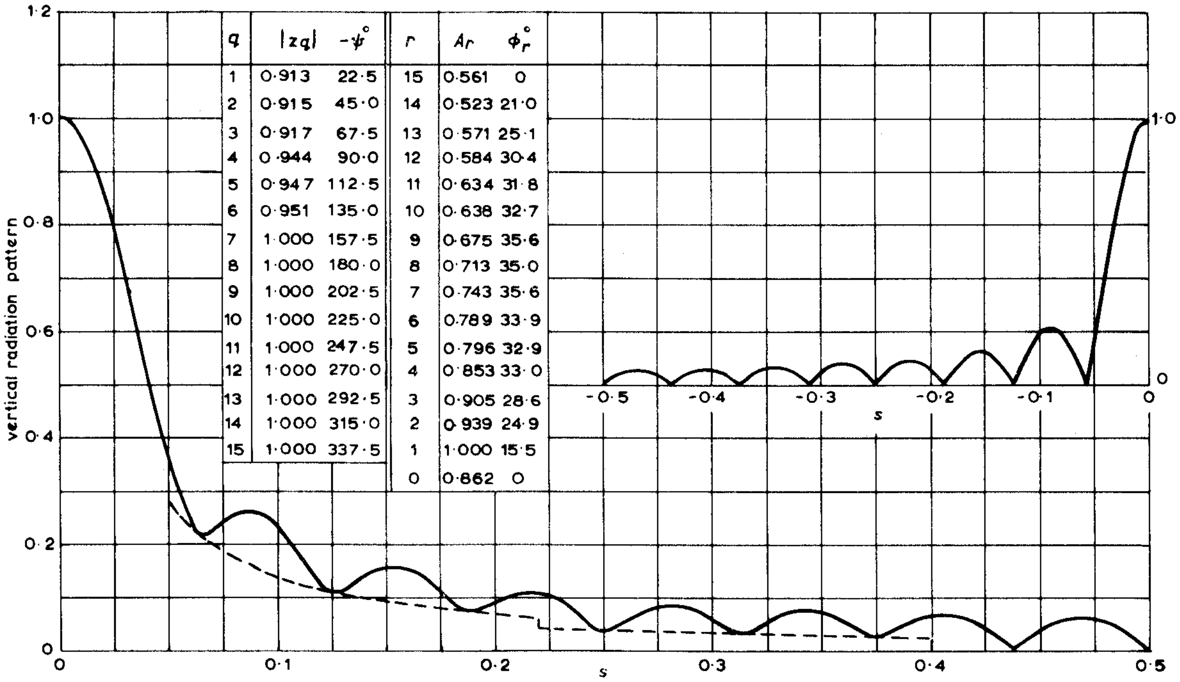

q	$\lvert z_q \rvert$	$-\psi°$	r	A_r	$\phi_r°$
1	0·913	22·5	15	0·561	0
2	0·915	45·0	14	0·523	21·0
3	0·917	67·5	13	0·571	25·1
4	0·944	90·0	12	0·584	30·4
5	0·947	112·5	11	0·634	31·8
6	0·951	135·0	10	0·638	32·7
7	1·000	157·5	9	0·675	35·6
8	1·000	180·0	8	0·713	35·0
9	1·000	202·5	7	0·743	35·6
10	1·000	225·0	6	0·789	33·9
11	1·000	247·5	5	0·796	32·9
12	1·000	270·0	4	0·853	33·0
13	1·000	292·5	3	0·905	28·6
14	1·000	315·0	2	0·939	24·9
15	1·000	337·5	1	1·000	15·5
			0	0·862	0

Fig. 14 - Computed v.r.p. for a 16λ array of isotropic sources: null-filling by polynomial-zero perturbation

- - - - - - - - null-filling reference, $m_q = 0{\cdot}70$ ($q = 1,2,3$), $m_q = 0{\cdot}50$ ($q = 4,5,6$), $m_q = 0$ ($q = 7, \ldots, 15$)

the current distribution I_r will be modified since it is determined by the product of complex factors (Equation (23)). The same argument holds if roots are inverted in combination so that the total number of solutions for $f(z)$ and hence also for the I_r is 2^t where t is the number of roots not lying on the unit circle. In the present application t is the actual number of filled nulls; if null-filling is complete, $t = N - 1$. It can be shown that the case in which all the non-unitary roots are inverted corresponds to a current distribution which is just an inverted and phase-reversed duplicate of the original distribution, i.e. $A_r' = A_{N-1-r}$ and $\phi_r' = -\phi_{N-1-r}$; this means that it is sufficient to compute only 2^{t-1} distributions.

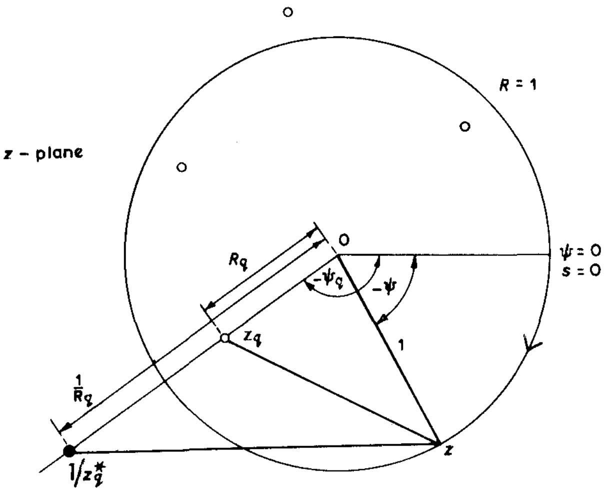

Fig. 15 - Polynomial root inversion on the z-plane

○ original root, z_q ● inverted root, $1/z_q^*$

In general, the other solutions cannot be found unless the polynomial roots are available and this means solving the complex equation $f(z) = 0$ which is of high degree[16]; with the polynomial-zero perturbation method of null-filling the roots are immediately available (Section 3.3.5).

An initial trial was made with a simple eight source array in which the first three nulls were filled to 75% by polynomial-root perturbation. There are eight different current distributions involved of which four need to be considered separately. They differ very little in their A– and ϕ– variation but the solution in which the roots alternate inside and outside the unit circle (i.e. roots 1 and 3 or root 2 inverted) gives the lowest maximum-to-minimum current ratio between sources.

A further example was a 16 source array with nulls 1, 2, 3 filled to 70% and nulls 4, 5, 6 filled to 50% by the above method (Fig. 14 shows the v.r.p.). The six filled nulls provide 32 current distributions for separate consideration. There is only a small spread in A–and ϕ– variations and also in 'vertical' impedance (described in Section 4.3). However, one solution (first zero inverted only) gives a significant reduction in the power difference between each half-array. In fact the power ratio becomes 0·94 compared with a figure of 0·39 for the design distribution.

The final example is an eight source array with null-filling by the twin-beam method. The required roots, obtained[†] from the original full quarter-sine distribution, are shown in Table 1; they all lie outside the unit circle and, except for the root at $\psi = \pi$ are in complex conjugate pairs. There are 36 current distributions to be considered and they show marked differences in A– variation; eight of the distributions are co-phased and the remainder show very small differences in ϕ– variation. Inversion of roots 1, 4 and 5 increase the minimum-to-maximum ratio of source currents from the original 0·098 to a maximum of 0·306. However, inversion of roots 2, 3 and 4 only slightly reduces this ratio to 0·297 (Table 1) but has the added advantage of increasing the power ratio between half-arrays to the maximum figure of 0·93; there is little variation in the input impedance of the array.

TABLE 1

Polynomial Roots and Current Distributions for an 8λ Array with Twin-Beam Null-Filling ($m = 1{\cdot}0$)

Original Roots			Distributions for original and inverted roots (2,3,4)			
q	R_q	ψ_q°	r	A_r	A_r	ϕ_r°
1	1·232	305·6	7	1·000	0·297	0
2	1·362	261·0	6	0·961	0·868	22·8
3	1·499	218·0	5	0·886	1·000	35·8
4	1·604	180·0	4	0·777	0·888	19·0
5	1·499	142·0	3	0·637	0·808	19·1
6	1·362	99·0	2	0·474	0·394	14·2
7	1·232	54·4	1	0·292	0·523	42·7
			0	0·098	0·313	0

Although there is no guarantee that null-filling designs can be optimized by polynomial-root inversion, the examples have shown that it is well worth while examining the associated current distributions; this applies especially if variable amplitude-and-phase solutions are being considered.

4. APPLICATION TO PRACTICAL TRANSMITTING AERIALS

The synthesis techniques described in Section 3 are for point-source arrays; nevertheless most of them can be readily applied to practical u.h.f. (and v.h.f.) transmitting aerials. Synthesis is performed by noting that the radiation pattern of a multi-tiered transmitting aerial of similar elements is given by the product of the pattern of one element and the pattern of the equivalent point-source array. The tiers may comprise simple vertical dipoles (BBC u.h.f. relay-station aerials) or, alternatively, simple horizontal dipoles grouped into identical 'panels' (BBC u.h.f. main-station aerials). In a practical design, important considerations apart from pattern shape (i.e. null-filling) are pattern bandwidth, aerial impedance and gain reduction.

[†] by J.W. Head.

4.1. Aerials with Individually-Fed Tiers

Low-power (relay) u.h.f. aerials and low- and high-power v.h.f. aerials are powered by feeding their tiers individually. For such aerials, null-filling is not normally required to be greater than about 50% and it should be obtained from a simple practical arrangement. These requirements suggest the use of the constant-amplitude method of phase perturbation for null-filling (Section 3.2.1). An example of the application of this method to the design of a u.h.f. relay aerial is described below.

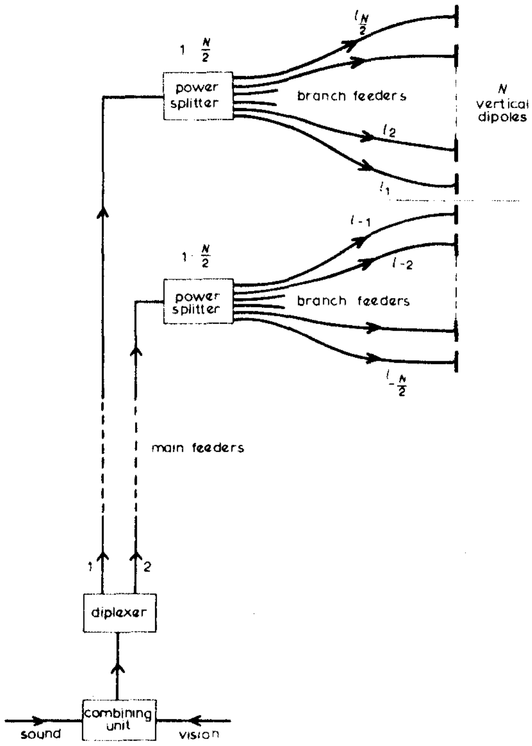

Fig. 16 - General arrangement of low-power u.h.f. aerial

A practical arrangement for a low-power aerial[17] is shown in Fig. 16. The aerial consists of vertical dipoles spaced 1·0λ apart; it is split into two halves, each half being branch-fed from an $N/2$: 1 power-splitting transformer. Cable lengths l_r are cut according to the required phase distribution ϕ_r (obtained from Equation (11)); since the transformers are placed below the aerial, the mean cable length must be made at least $N\lambda$. The diplexer is at ground level so that with a typical 45 m (150 ft) tower, the main feeder lengths are about 52 m (170 ft); using conventional cables at 500 MHz this means that the diplexer and transformers are separated by about 100λ.

If such an aerial were uniformly fed, its v.r.p. would be given by $g(\theta)P(\theta)$ where $g(\theta)$ is the v.r.p. of a single tier and $P(\theta)$ is given by Equation (1). It therefore follows that the point-source synthesis procedure of Section 3.2.1 may be applied provided the null-filling amplitudes m_q are inversely weighted by the factor $g(\theta)$. For half-wave dipoles, we set

$$m'_q = \frac{(N^2 - q^2)^{\frac{1}{2}}}{N\cos(\pi q/2N)}\, m_q \qquad (26)$$

in Equation (11) where m_q is the intended null-filling level.

In a typical 16-tier aerial, the null-filling was specified as $m \nless 0{\cdot}50$ for $\theta_0 < \theta < \pi/12$ and $m \nless 0{\cdot}25$ for $\pi/12 < \theta < 5\pi/36$. The non-oscillatory, rather than the oscillatory, solution for determining ϕ_r was employed because it gave a v.r.p. with sufficient latitude to allow the specification to be satisfied over the required bandwidth (±10%); moreover, the associated aerial impedance matching was slightly superior. Differential phase correction 2Λ, derived from Equation (12) was found to be 36° but this figure was actually increased to 50°, with negligible deterioration of the v.r.p., in order to reduce the aerial mismatch still further (the mechanism of this reduction is explained in Section 4.3). Beam-tilt was required to be 1·75° so that an additional progressive phase-shift of 5° per tier was superposed on the phase distribution.

The centre-frequency and end-of-band v.r.p.s for the 16-tier aerial are shown in Fig. 17 together with the null-filling specification for the pattern; null-filling is very satisfactory and there is some latitude at the pattern minima which gives the v.r.p.s some resistance to the effects of phase errors. Gain reductions for the patterns shown are 0·7 dB (f_0), 0·5 dB (0·9f_0) and 0·8 dB (1·1f_0).

Apart from random phase errors* which occur by inaccurate cutting of branch-feeders to the distribution ϕ_r, a split aerial system (e.g. Fig. 16) may introduce a differential phase error between array halves either through cutting inaccuracies of the main feeders or through differential thermal expansion between them. This error can be as high as ±10° if the temperature difference between feeders is about 20°C; computation has shown that the null-filled v.r.p.s in the above example remain satisfactory up to this error limit.

---

* Section 4.4 gives a brief discussion of the effects of random errors in l_r.

It has been shown that the phase perturbation (non-oscillatory solution) method for null-filling is very adaptable to the design of individually fed multi-tiered transmitting aerials. If null-filling is restricted to a small number of null-points, as it is at v.h.f., it is preferable to use the alternative oscillatory solution.

4.2. Panel-Aerials

At high-power u.h.f. stations with horizontal polarization, the preferred inter-tier spacing is about 0·5λ and it is then practicable to build up the aerial from standard vertical groups or panels of horizontal dipoles. Typical panels are 2 to 4λ long; a 4λ panel, for example, would carry eight dipoles spaced 0·5λ apart and 0·25λ away from a reflecting screen, where λ is the wavelength at the design frequency. Columns of panels are mounted around the mast axis; the individual columns are normally split into vertical sections for operational reasons and usually fed with progressive phase-shift around the mast in order to produce an arrangement which provides a good horizontal radiation pattern (h.r.p.) and an acceptable impedance characteristic.

4.2.1. General Considerations

We concern ourselves here with the v.r.p. from a single column of panels. Synthesized current distributions will be considered that are subject to the restriction that the A and ϕ components over every panel must be identical, since the complexities arising from special amplitude and phase adjustments within each panel are to be avoided if possible. Amplitude variation of the aerial current distribution can be provided, if necessary, from power-splitting transformers (e.g. hybrid units); phase variation can be obtained from a branch-feeder system similar to that described previously (Section 4.1).

In panel-aerials the current distributions required for null-filling and beam-tilt must be approximated by an array of sources spaced 2 to 4λ apart. The amplitude component A_r is best realized by allowing each panel to carry the same power as that carried by all the equivalent sources contained in its length (this problem is avoided if we adopt a synthesis method in which the amplitude component can be specified at the outset as a 2 to 4λ stepped

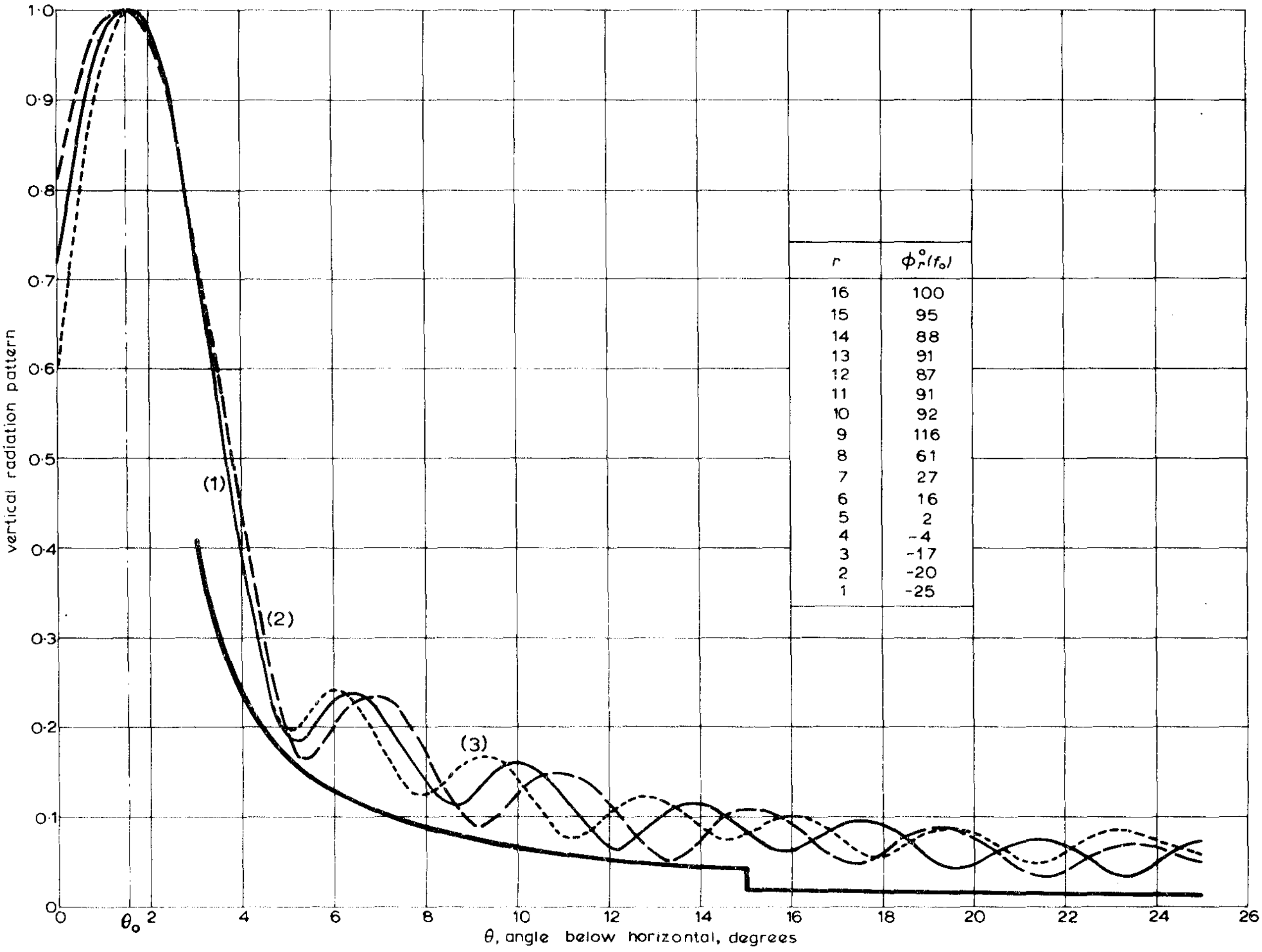

r	$\phi^\circ_r(f_o)$
16	100
15	95
14	88
13	91
12	87
11	91
10	92
9	116
8	61
7	27
6	16
5	2
4	-4
3	-17
2	-20
1	-25

Fig. 17 - Computed v.r.p.s for a 16-tier relay aerial with vertical half-wave dipoles spaced 1·0λ apart at f_O: null-filling by phase perturbation (non-oscillatory solution), $\Delta = 25°$

(1) ———— f_O, centre-frequency, (2) — — — — $0{\cdot}9f_O$, (3) - - - - - - - - $1{\cdot}1f_O$

———— null-filling specification, $m = 0{\cdot}50/0{\cdot}25$

distribution). Realization of the phase component ϕ_r generally involves electrical phasing of the panels together with some mechanical stagger (i.e. panel-tilt). Panel-tilt is normally required over those parts of the aerial where the variation is sharp in order to ensure good pattern accuracy. The point-source methods of synthesis described in Section 3 can be used as follows.

(i) The aperture distribution is calculated as if it were a non-panel aerial, allowance being made for the reflecting screen, i.e. the v.r.p. of each source-image combination $h(\theta)$ is taken into account

(ii) Each panel is driven with the same power and average phase of the sources it replaces; if the phase variation is very large, panel-tilt is also employed.

The procedures of Section 3 can therefore be applied provided that the null-filling amplitudes are inversely weighted by the screen-factor $h(\theta)$. For dipoles placed 0·25λ away from the screen, we set

$$m_q' = m_q / \sin(\frac{\pi}{2}\cos\theta) \qquad (27)$$

in the design equations where m_q' is the intended null-filling level.

Starting from a sampled distribution ϕ_r (1·0λ spacing) the electrical phases of the panels Φ_r are taken as the mean of the phases of the sources contained by the panel, i.e.

$$\begin{aligned} \Phi_r &= \tfrac{1}{2}(\phi_{2r} + \phi_{2r-1}) && [2\lambda \text{ panel}] \\ \Phi_r &= \tfrac{1}{4}(\phi_{4r} + \phi_{4r-1} + \phi_{4r-2} + \phi_{4r-3}) && [4\lambda \text{ panel}] \end{aligned} \qquad (28)$$

A 4λ panel is illustrated in Fig. 18(*a*). Panel-tilts, where required, are determined accurately enough by the differential phase-shift between the outermost sources contained by the panel. The mechanical tilt-angles $\Phi_r^{(m)}$ are given by

$$\begin{aligned} \Phi_r^{(m)} &= \frac{1 \cdot 07}{2\pi}(\phi_{2r} - \phi_{2r-1}) && [2\lambda \text{ panel}] \\ \Phi_r^{(m)} &= \frac{1 \cdot 07}{6\pi}(\phi_{4r} - \phi_{4r-3}) && [4\lambda \text{ panel}] \end{aligned} \qquad (29)$$

These angles have been increased by 7% in order to allow for the fact that equivalent electrical phasing produced by source-stagger (i.e. panel-tilt) is reduced by the factor $\cos\theta$ at declinations from the horizontal; the weighting factor 1·07 provides accurate equivalence at $\theta \simeq 20°$ and equal errors at $\theta = 0$ (over null-filling) and at $\theta = 30°$ (under null-filling).

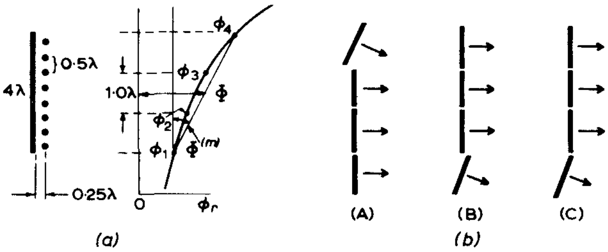

Fig. 18 - Principles of panel-tilt

(*a*) realization of phase distribution for a 4λ panel
(*b*) alternative panel-tilt arrangements: (A), leading ϕ_r; (B), (C), lagging ϕ_r

It is sometimes preferable to use the negative inverted phase distribution $-\phi_{N-r+1}$ (i.e. lagging) so that the largest phase-slopes ϕ' which normally appear at the end(s) or centre of the aerial can be realized with panels tilted away from the main array. Thus in Fig. 18(*b*) arrangement B based on an inverted phase distribution is preferred to the arrangement A that results from the initial distribution. The advantage is that an arrangement such as B will give less inter-panel mutual coupling and makes realization somewhat easier. In practice, it may be more convenient to tilt a panel about its end-point (arrangement C) rather than its centre-point; provided that the electrical phase of the panel is suitably adjusted, the previous results (Equation (29)) also apply to this situation.

4.2.2. Design Examples

An example of the application of the phase-perturbation method (Section 3.2.1) to null-filling a 20λ panel-aerial is given in Fig. 19 which shows computed v.r.p.s at three frequencies (f_0, 0·9f_0 and 1·1f_0); the non-oscillatory solution has been used with m = 0·50, and Δ = 20° with beam-tilt set to θ_0 = 0·5°. It is seen that the approximation of tilting the central panels only ($\Phi_{5,6}^{(m)} = \pm 6 \cdot 5°$) is quite justified. Gain reductions for the cases shown are 0·48 dB (f_0), 0·81 dB (0·9f_0) and 0·37 dB (1·1f_0). If the oscillatory solution is used instead, panel-tilt can be restricted to the end panels (1 and 10) and it is found that the v.r.p.s remain satisfactory at f_0 if this tilt is further restricted to either the upper panel (10, leading distribution) or the lower panel (1, lagging distribution); however, for frequencies away from f_0 some v.r.p. minima fall on or below the null-filling specification. The results given here have shown that phase perturbation can give satisfactory 50% null-filling over a ±10% frequency band without excessive sidelobe maxima or gain reduction.

An alternative constant-amplitude technique for null-filling with panel-aerials is supplied by the stationary-phase method (Section 3.2.2). Fig. 20 shows computed v.r.p.s for a 32λ aerial comprising eight 4λ panels in which the logarithmic (lagging) phase distribution (obtained by setting k = 0·54, s_1 = 0·0089 and s_2 = 0·50 in Equation (15)) has been approximated by panel phasing and tilting.

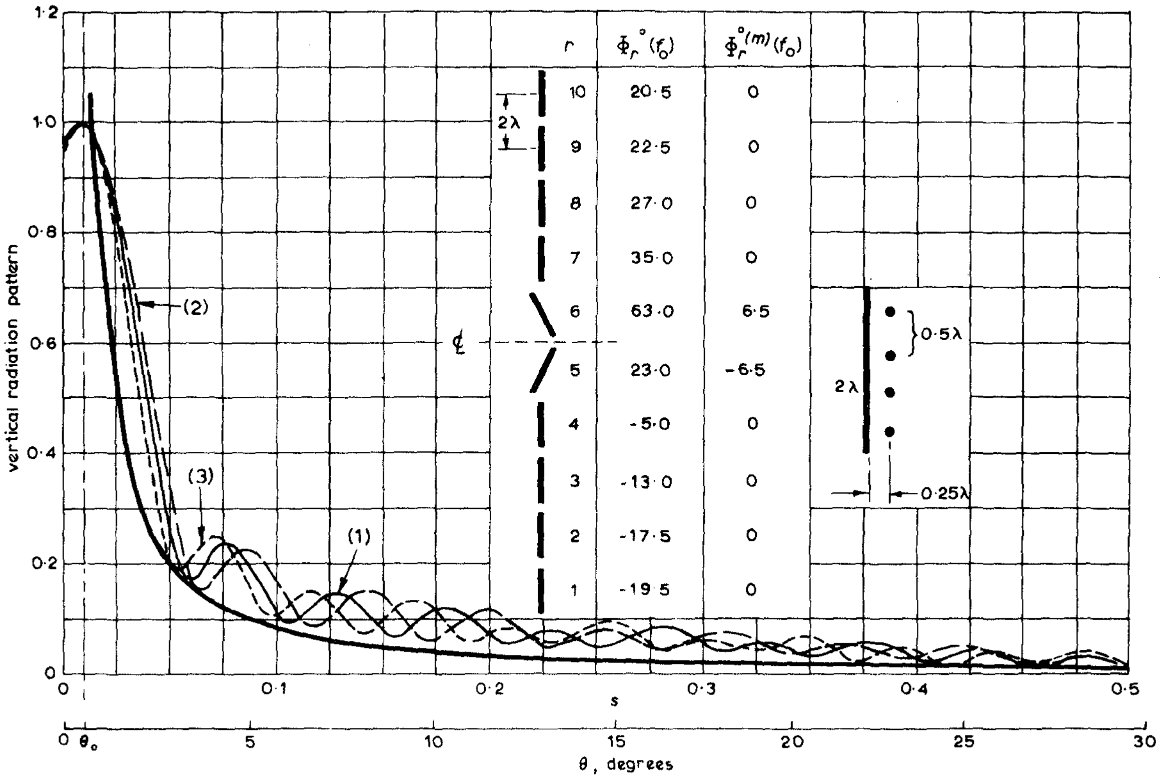

r	$\Phi^\circ_r(f_0)$	$\Phi^{\circ(m)}_r(f_0)$
10	20·5	0
9	22·5	0
8	27·0	0
7	35·0	0
6	63·0	6·5
5	23·0	-6·5
4	-5·0	0
3	-13·0	0
2	-17·5	0
1	-19·5	0

Fig. 19 - Computed v.r.p.s for 10 panel, 20λ aerial with 4 horizontal dipoles/panel: null-filling by phase perturbation (non-oscillatory), Δ = 20°

(1) ——— f_0, centre-frequency, (2) — — — — $0{\cdot}9f_0$, (3) - - - - - - $1{\cdot}1f_0$

▬▬▬ null-filling specification, $m = 0{\cdot}50$

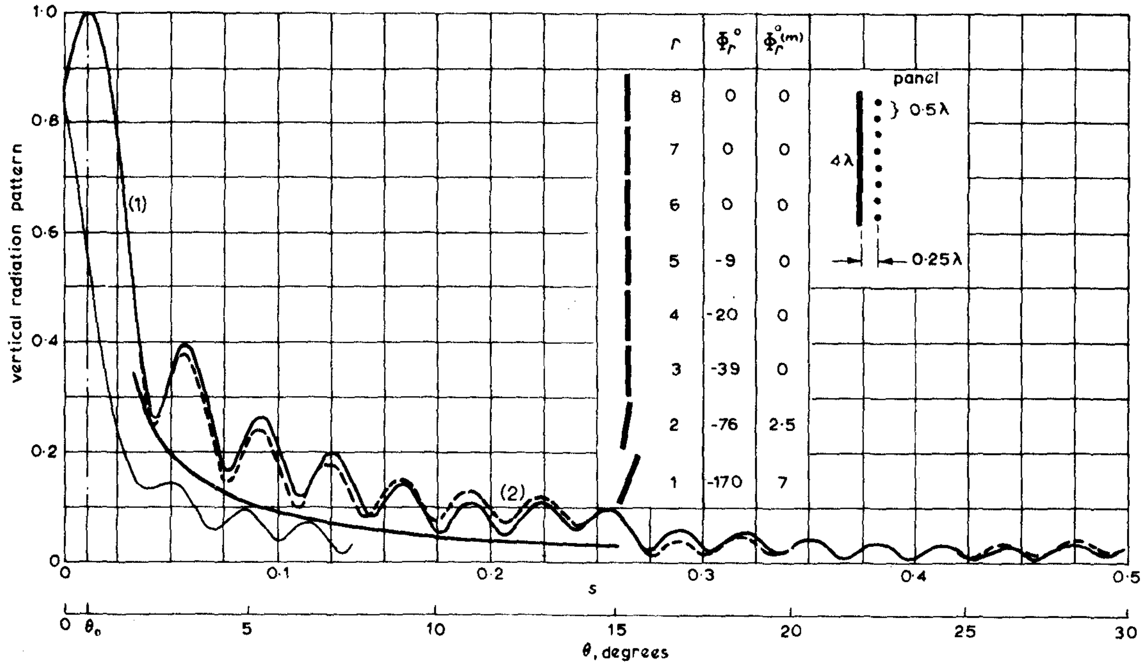

r	Φ°_r	$\Phi^{\circ(m)}_r$
8	0	0
7	0	0
6	0	0
5	-9	0
4	-20	0
3	-39	0
2	-76	2·5
1	-170	7

Fig. 20 - Computed v.r.p.s for 8 panel, 32λ aerial with 8 horizontal dipoles/panel spaced 0·5λ apart; null-filling by the stationary-phase method, k = 0·54

(1) ——— v.r.p. for arrangement shown (2) - - - - - - v.r.p. with panel 1 (lower) tilted only

▬▬▬ null-filling specification, $m = 0{\cdot}75$

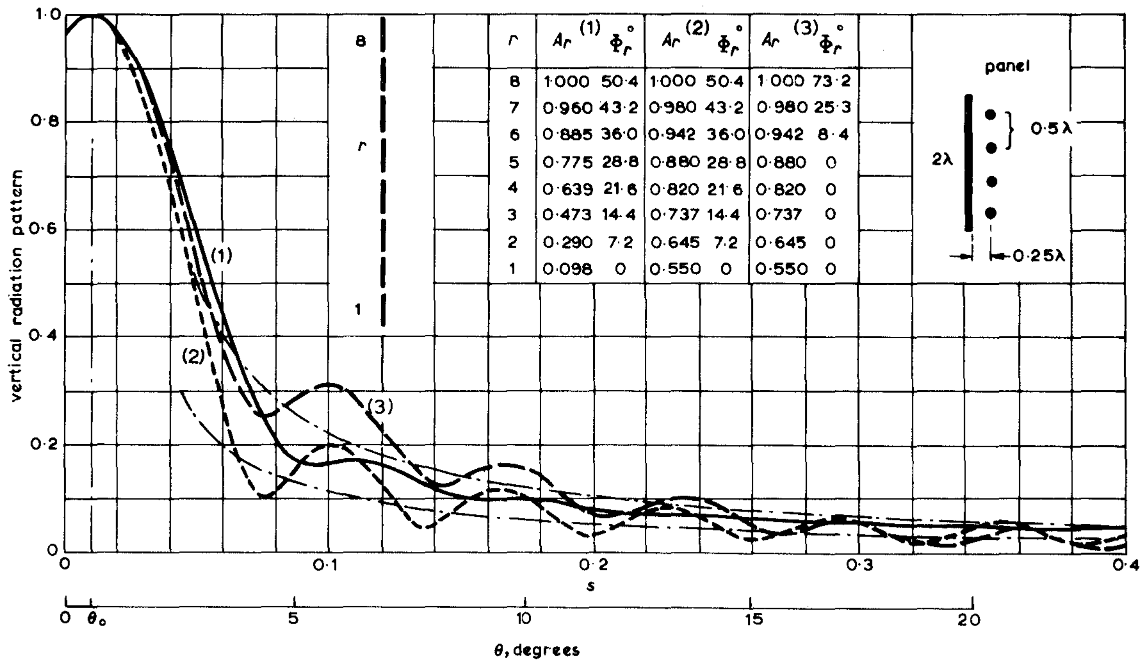

r	$A_r^{(1)}$	Φ_r°	$A_r^{(2)}$	Φ_r°	$A_r^{(3)}$	Φ_r°
8	1·000	50·4	1·000	50·4	1·000	73·2
7	0·960	43·2	0·980	43·2	0·980	25·3
6	0·885	36·0	0·942	36·0	0·942	8·4
5	0·775	28·8	0·880	28·8	0·880	0
4	0·639	21·6	0·820	21·6	0·820	0
3	0·473	14·4	0·737	14·4	0·737	0
2	0·290	7·2	0·645	7·2	0·645	0
1	0·098	0	0·550	0	0·550	0

Fig. 21 - Computed v.r.p.s for 8 panel, 16λ aerial with 4 horizontal dipoles/panel spaced 0·5λ apart: null-filling by the twin-beam and stationary-phase methods

(1) ———— quarter-sine distribution (2) - - - - - - - quarter-sine/pedestal distribution
(3) — — — — phased quarter-sine/pedestal distribution —·—·—·— null-filling specification, $m = 0{\cdot}50/1{\cdot}0$

The 'jump' in the v.r.p. near $s = 0{\cdot}25$ is due to the coarse quantization of the original distribution into 4λ groups; this jump is accentuated if panel-tilt is restricted to the lowest panel only (broken curve). Effective null-filling is satisfactory ($m > 0{\cdot}75$ for $0 < s < 0{\cdot}25$) although the sidelobe maxima are rather high and the v.r.p. minima are too large near $s = 0{\cdot}1$; nevertheless, the maximum ratio of adjacent v.r.p. maxima and minima is not greater than 6 dB in the important range and this would normally be satisfactory. The loss of aerial gain due to de-phasing is about 1·4 dB. There is little advantage in replacing panels 1 and 2 (Fig. 20) with four 2λ panels and tilting all or some of these; the major effect is that the v.r.p. minima are slightly elevated in the range $0{\cdot}25 < s < 0{\cdot}50$.

The twin-beam method of pattern shaping (Section 3.1.2) can also be adapted to null-filling the v.r.p.s of panel-aerials. Fig. 21 shows some computed results obtained for a 16λ aerial with eight panels. Curve (1) is the smooth cosecant pattern derived from a sampled quarter-sine-wave amplitude distribution (the variation in Φ_r is for beam-tilt); the amplitude variation, however, is rather high ($A_8/A_1 > 10$). Curve (2) is the v.r.p. obtained by introducing a superposed pedestal distribution of equal amplitude ($b = 1$); amplitude variation has been reduced ($A_8/A_1 < 2$) but the v.r.p. minima now fall below the limit $m = 0{\cdot}5$. The null-filling can be corrected by using the stationary-phase method (Section 3.3.4) to synthesize a cosecant pattern from such an amplitude distribution. Curve (3) shows the v.r.p. obtained using this method. The phase distribution Φ_r was derived by numerically integrating the expression for $\phi'(x)$ obtained from the synthesis equation (Equation (14) modified for variable $A(x)$); Φ_r is co-phased over the lower five panels through beam-tilt adjustment ($\theta_0 = 0{\cdot}6^{\circ}$). Null-filling is now satisfactory up to $\theta = 15^{\circ}$ but falls off rapidly for larger declinations. The gain reductions for the three cases are 0·90 dB (curve 1), 0·13 dB (curve 2) and 0·52 dB (curve 3).

The amplitude variation demanded by the twin-beam method is not realizable with simple power-splitting devices. Stepped approximations to quarter-sine-wave amplitude distributions, however, can be obtained from simple arrangements of diplexer and triplexer units. Fig. 22 shows two suggested practical arrangements* for eight-panel aerials. Arrangement (*b*), employing five diplexers and one triplexer was found to give slightly superior results and will be used as the basis of further design examples which are described below.

Starting from the three-step amplitude distribution of Fig. 22(*b*), panel-phases were derived by the stationary-phase method following the procedure given in Section 3.3.4; the parameters were set to $k = 0{\cdot}51$, $s_1 = 0{\cdot}0156$ and $s_2 = 0{\cdot}5$. The resulting phase distribution and v.r.p. are shown in Fig. 23 (curve 1) for $\theta_0 = 0{\cdot}6^{\circ}$; the uppermost panel, number eight, has been tilted 8° downwards as required by the phase profile (Equation (29)). If panel-tilting is avoided, the v.r.p. minima fall below $m = 0{\cdot}5$ beyond $\theta = 10°$ as shown by curve (2); for comparison, the v.r.p. obtained from the stepped A_r distribution alone (the variation in Φ_r is for beam-tilt) is also shown (curve 3). Gain reductions for the three cases are 0·65 dB (curve 1), 0·51 dB (curve 2) and 0·13 dB (curve 3). The null-filling for large declinations is rather high (Fig. 23, curve 1) and the gain reduction unnecessarily large. By reducing the beam-tilt on the uppermost panel, these pattern minima can be lowered to a satisfactory level. Fig. 24 shows computed v.r.p.s for a practical 16λ aerial designed to radiate in u.h.f. Channels 26 and 33; the previous distribution with a reduced panel-tilt of 4°(downwards) has been used at the centre-frequency $f_0 = 542{\cdot}25$ MHz (mid-point of Channels 26 and 33). The computed v.r.p.s shown in Fig. 24 are for Channel 33, vision (curve 1) and sound (curve 2), and also the centre-frequency case curve (3). The design satisfies the pattern specification given in the figure; gain reductions at the three frequencies are 0·39 dB (curve 1), 0·35 dB (curve 2) and 0·54 dB (curve 3).

---

* due to J.L. Eaton.

A final design example is given in Fig. 25 which shows computed v.r.p.s for an eight panel, 16λ aerial with current distributions A_r, Φ_r designed by the current-perturbation ('Woodward-quadrature') method (Section 3.3.3). The original distribution was determined from Equation (19) for $m_q = 0{\cdot}75$, $q = 1,2,3,4$ and 5; both oscillatory (curve 1), and non-oscillatory (curve 2) null-filling solutions have been explored with neither solution requiring panel-tilt for accurate realization. The v.r.p. given by the oscillatory solution (curve 1) is satisfactory with regard to both null-filling and sidelobe level; the gain reduction for both solutions is 0·34 dB.

Results similar to that given in the previous example (Fig. 25, curve 1) can be obtained by the polynomial-root perturbation method (Section 3.3.5), again without employing panel-tilt; the null-filling obtained is slightly more accurate. This method suffers the same disadvantage, however, that the

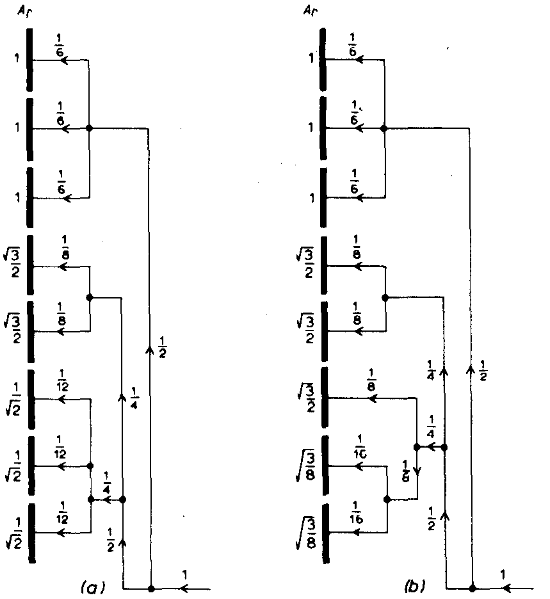

Fig. 22 - Practical arrangements for aerial with 8 panels: approximations to quarter-sine/pedestal amplitude distribution; numbers against feeders indicate power ratios

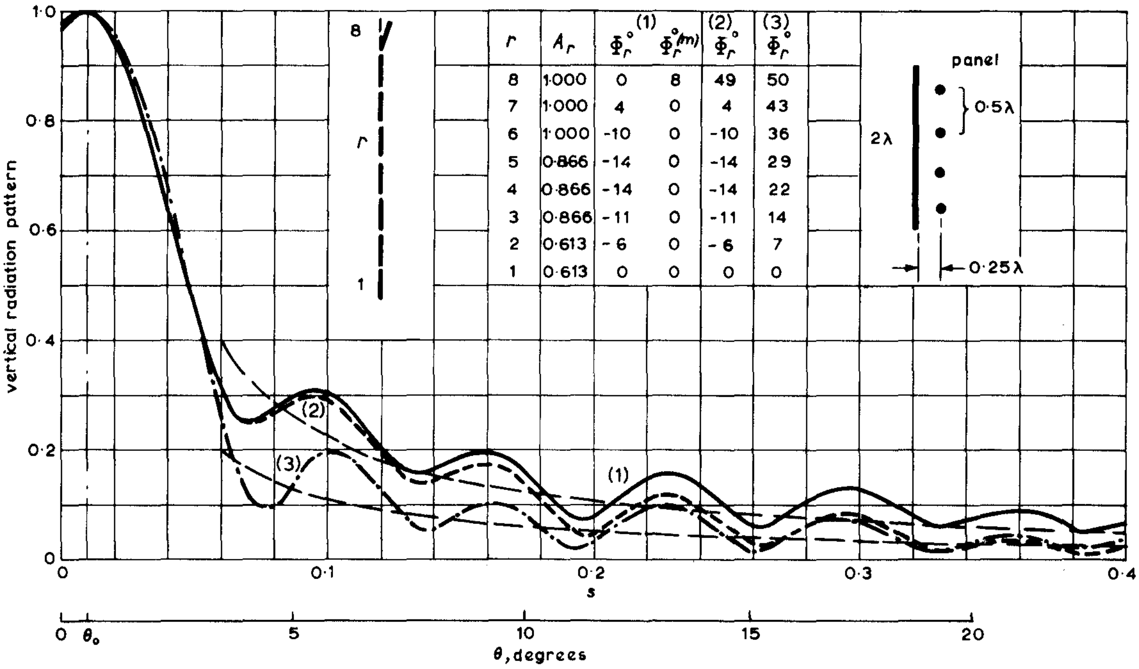

r	A_r	(1) Φ_r°	(1) $\Phi_r^{\circ(m)}$	(2) Φ_r°	(3) Φ_r°
8	1·000	0	8	49	50
7	1·000	4	0	4	43
6	1·000	-10	0	-10	36
5	0·866	-14	0	-14	29
4	0·866	-14	0	-14	22
3	0·866	-11	0	-11	14
2	0·613	-6	0	-6	7
1	0·613	0	0	0	0

Fig. 23 - Computed v.r.p.s for 8 panel, 16λ aerial with 4 horizontal dipoles/panel spaced 0·5λ apart: null-filling by stationary-phased practical current distribution

(1) ———— v.r.p. with panel 8 tilted (2) - - - - - - - v.r.p. with no panel-tilt

(3) -·-·-·- v.r.p. with amplitude distribution only — — — null-filling specification, $m = 0{\cdot}50/1{\cdot}0$

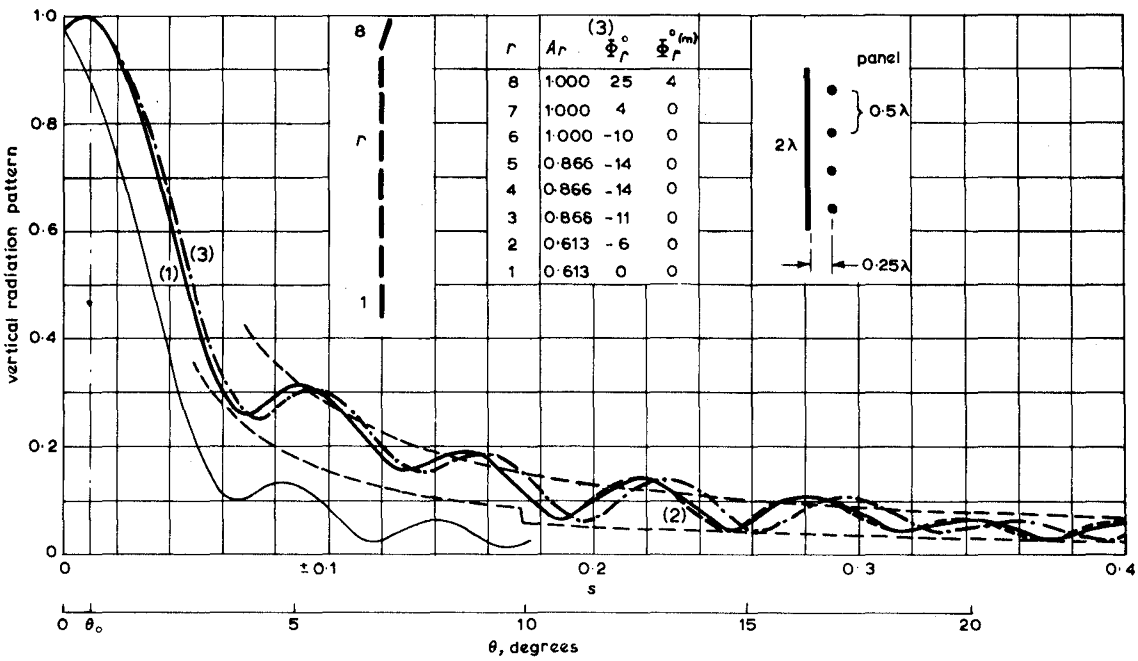

r	(3) A_r	(3) Φ_r°	$\Phi_r^{\circ(m)}$
8	1·000	25	4
7	1·000	4	0
6	1·000	-10	0
5	0·866	-14	0
4	0·866	-14	0
3	0·866	-11	0
2	0·613	-6	0
1	0·613	0	0

Fig. 24 - Computed v.r.p.s for 8 panel, 16λ aerial with 4 horizontal dipoles/ panel spaced 0·5λ apart: null-filling by stationary-phased practical current distribution

(1) ———— v.r.p. for f = 567·25 MHz (Channel 33 vision) (2) – – – – – – v.r.p. for f = 573·25 MHz (Channel 33 sound)

(3) —·—·—·— v.r.p. for f_0 = 542·25 MHz (Channels 26/33 mid-point)

— — — — pattern specification, m = 1·25 (upper limit)

m = 0·7/0·5 (lower limit)

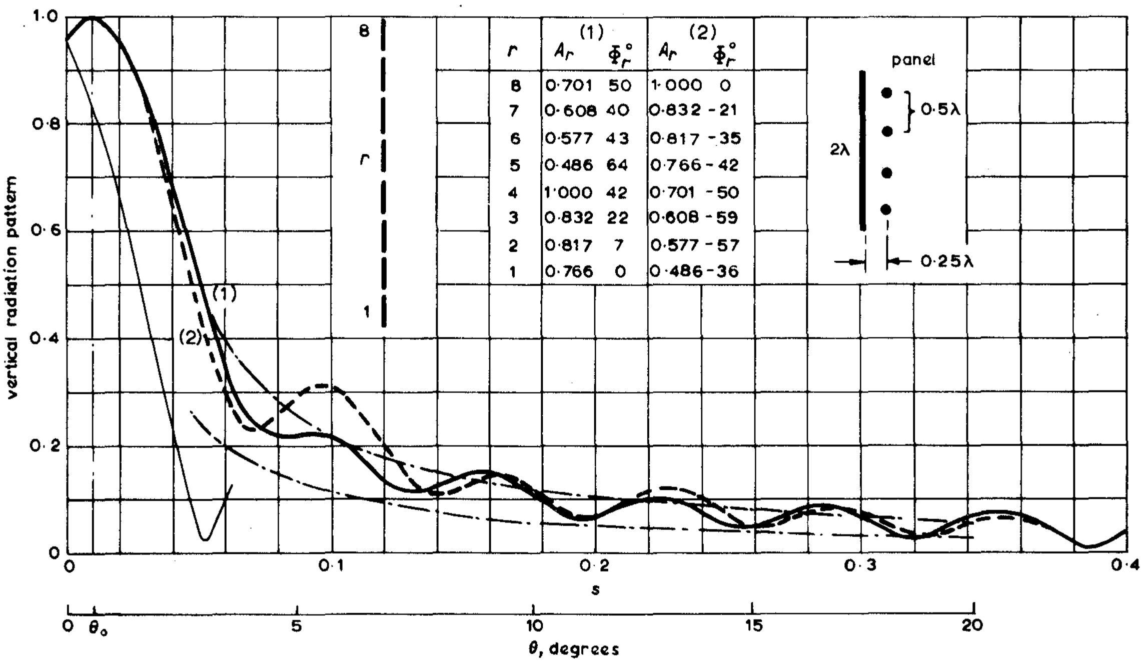

r	(1) A_r	(1) Φ_r°	(2) A_r	(2) Φ_r°
8	0·701	50	1·000	0
7	0·608	40	0·832	-21
6	0·577	43	0·817	-35
5	0·486	64	0·766	-42
4	1·000	42	0·701	-50
3	0·832	22	0·608	-59
2	0·817	7	0·577	-57
1	0·766	0	0·486	-36

Fig. 25 - Computed v.r.p.s for 8 panel, 16λ aerial with 4 horizontal dipoles/panel spaced 0·5λ apart: null-filling by current perturbation ('Woodward-quadrature') with no panel-tilting

(1) ———— oscillatory solution (2) – – – – – – non-oscillatory solution

—·—·—·— null-filling specification, m = 0·5/1·0 synthesized amplitude distribution cannot be easily realized with a simple practical arrangement. Nevertheless, with the associated polynomial roots available, the other solutions can be found directly and one or more of these may be more amenable to simple realization than the parent solution.

4.3. Aerial Impedance Compensation

The conventional method of obtaining good aerial impedance matching over a wide bandwidth is to progressively phase rotate the feed to each horizontal group of tiers around the mast axis ('horizontal' impedance compensation). The main disadvantage of this form of impedance compensation is that it is generally impractical to obtain simultaneously good directional h.r.p.s. It would obviously be advantageous if good impedance matching could be achieved by feeding the aerial tiers in vertical rather than horizontal groups since the h.r.p. and impedance adjustments become independent of one another. Aerial current distributions designed to provide null-filled v.r.p.s include a phase-varying component (if only to supply the beam-tilt) so that, in general, 'vertical' impedance compensation is possible; for any given distribution, the degree of compensation will depend on the grouping of the tiers. For low-power (relay) aerials null-filled by phase perturbation (arrangement shown in Fig. 16), good compensation can be obtained simply by feeding the half-aerials from a 90°-diplexer[11,17]. A similar method for obtaining good impedance matching in a high-gain aerial null-filled by the twin-beam method has also been proposed[18].

The problem of optimizing the selection of groups of tiers in one stack for vertical impedance compensation is beyond the scope of this report. However, there is an important and useful general relation between the v.r.p. on the one hand and impedance matching of a group of contiguous tiers which is easily demonstrated. If we consider, for example, the grouping arrangement shown in Fig. 26, it can be shown that the input reflexion coefficient at the diplexer is given by

$$|\rho_{in}| \simeq |\rho| \left| \frac{\sum_{1}^{N} A_r^2 \exp(j2\phi_r)}{\sum_{1}^{N} A_r^2} \right| \qquad (30)$$

where ρ is the reflexion coefficient of the branch-feeder terminations (dipoles or panels) assumed equal and $A_r \exp j\phi_r$ is the current distribution over the group; this expression for ρ_{in} ignores inter-tier mutual impedance and mismatch in the power-splitting transformers. Equation (30) shows that $|\rho_{in}|$ is proportional to the field which would be radiated *horizontally* if the current distribution over the aperture were squared. Now the radiation pattern of the squared distribution resembles the actual v.r.p., the principal difference being that the beam-tilt is approximately doubled. Consequently $|\rho_{in}|$ will generally be small if the whole of the main lobe of the 'squared' radiation pattern lies below the horizontal.

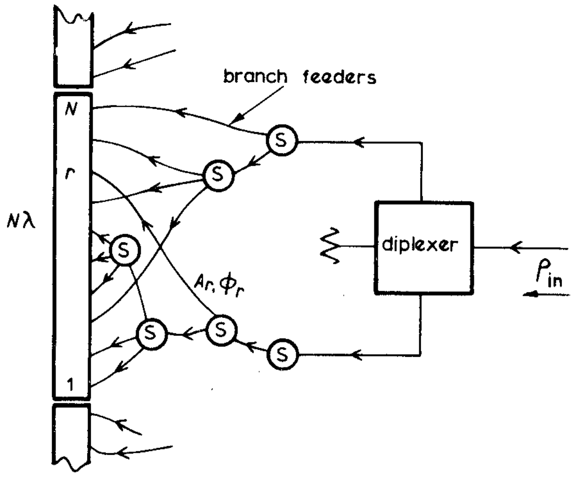

Fig. 26 - Vertical impedance compensation by tier-grouping and power splitting. S: power-splitting transformers

The relationship between the effective reflexion coefficient $|\rho_{in}|$ and the actual v.r.p. above the horizontal is closest for constant-amplitude distributions. A good example is shown in Fig. 27. Curve (1) is the v.r.p. above the horizontal of a 32λ aerial, null-filled by the stationary-phase method and with the inherent beam-tilt removed, while curve (2) is the radiation pattern of the corresponding squared distribution. If a progressive phase shift is added to the distribution to introduce beam-tilt, both curves will move to the left but curve (2) will

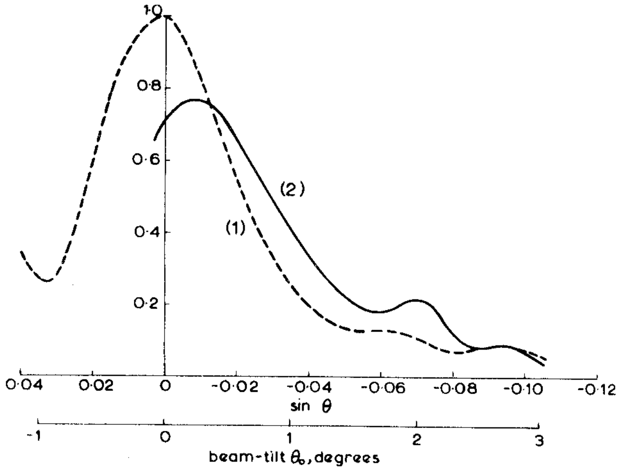

Fig. 27 - Variation of input matching $|\rho_{in}/\rho|$ with beam-tilt θ_0 for a 32λ aerial null-filled by the stationary-phase method: comparison with v.r.p. above the horizontal

(1) - - - - - - v.r.p. above the horizontal
(2) ———— v.r.p. of squared distribution

move twice as far as curve (1). Thus if the beam-tilt of the actual v.r.p. is θ_0 the field radiated in the horizontal direction by the squared distribution, which is equal to the value of $|\rho_{in}/\rho|$ for this particular value of θ_0, is given by the height of curve (2) at $\sin\theta = \sin 2\theta_0$. If the $\sin\theta$ scale is replaced by a θ_0 scale, curve (2) also shows how $|\rho_{in}/\rho|$ varies with beam-tilt.

Because of the similarity of the two patterns, the value of beam-tilt required to obtain a low value of $|\rho_{in}|$ can be inferred from the actual v.r.p. above the horizontal without actually calculating the pattern of the squared distribution. In the example shown the actual untilted pattern falls to a low value at $\sin\theta = -0{\cdot}05$ ($\theta = -3^\circ$); a beam-tilt of $1{\cdot}5^\circ$ is therefore sufficient for a low value of $|\rho_{in}|$ to be obtained.

It is rarely practicable to increase beam-tilt in order to achieve good impedance matching (as was effectively done for the relay aerial design, Section 4.1) nevertheless, it is theoretically possible to achieve good impedance compensation by over-tilting the v.r.p. with electrical phasing and re-adjusting to the desired beam-tilt by staggering the sources, for example by using panel-tilt. Finally, experiment has shown that the other current distributions derived from polynomial-root inversion (Section 3.4) offer no worthwhile reductions in impedance mismatch.

4.4. Practical Limitations

Current distributions for null-filled v.r.p.s are realized by energizing the aerial elements (dipoles or panels) from common drive-points or power-splitting transformers via branch-feeders (Figs. 16 and 26). The intended amplitude distribution is normally either constant or stepped and accurately realizable with simple power-splitters (e.g. Fig. 22); the prescribed phase distribution, however, is realized in the branch-feeder system which is frequency sensitive and the process of cable cutting can introduce random phase errors. In addition, the actual current distribution will be in error in amplitude and phase because of inter-tier mutual coupling. Errors due to mutual coupling are calculable and, if necessary, the v.r.p. given by the known resultant current distribution can be checked by computation; the effects of random phase errors, however, must be examined statistically (see, for example, Ref. 11).

With vertical polarization (low-power aerials) the mutual coupling between dipoles is very small and may be neglected. For horizontal polarization (high-power aerials) mutual coupling cannot be completely neglected; although inter-panel coupling would not normally exceed 5 to 10% there will be large inter-dipole coupling within each panel which must be allowed for in their design. The largest errors due to inter-panel coupling are likely to occur near the ends of the aerial where the tiers are not uniformly surrounded by other tiers, and also over those parts of the aperture where A_r and Φ_r vary rapidly. Lagging phase distributions are to be preferred since the tilted panels can then be faced away from the main column of panels (e.g. Fig. 18(*b*), arrangements B and C). Large variations in ϕ_r or Φ_r can be reduced by exchanging electrical phase for source stagger (as in panel-tilting). In fact if the entire phase distribution is simulated by horizontally staggering the tiers (and tilting panels where required) computation has shown that the resulting null-filled v.r.p.s remain entirely satisfactory. Furthermore, with such an arrangement, errors due to mutual coupling can be completely removed if all branch-feeders are cut in length to an odd multiple of a quarter-wavelength; this would only be possible, however, for single-channel working.

Random phase-errors due to feeder-cutting inaccuracies will either increase or decrease null-filling in the v.r.p. depending on the relative amplitude and phase of the contribution from the errors at the null-points. The standard deviation of the phase errors should not normally exceed 10°. Practical experience with the 16λ relay aerial described in Section 4.1 showed that the theoretical v.r.p.s determined from measured current distributions remained within specification up to large declinations where the pattern is most sensitive to phase errors. This result indicates that feeder-cutting accuracies in excess of that corresponding to a 10° standard deviation can be achieved in practice.

The main conclusion is that it is perfectly feasible to realize null-filling current distributions quite accurately; random phase-errors can be minimized by careful feeder cutting and errors due to inter-tier mutual coupling can be reduced to an insignificant level by choosing a suitable combination of source-stagger and electrical phasing over the aerial.

Finally, it is noted that the sensitivity of the v.r.p. to frequency departures from the design- or centre-frequency depends on what fraction of the null-filling is due to the phase component of the current distribution and also, to a lesser extent, on the diplexing arrangement employed. In general, pure amplitude distributions (e.g. the co-phased quarter-sine-wave distribution required by the twin-beam method) are reasonably insensitive to frequency variation, in realization. The first-order effect of a change in frequency is that null-filling increases for $f > f_0$ and decreases for $f < f_0$; beam-tilt remains sensibly constant since the source spacing and phasing vary together in proportion. Computation has shown that pattern bandwidth is no problem for frequency variations up to about ±10% with the practically usable null-filling schemes.

5. FINAL REMARKS AND CONCLUSIONS

Faced with the problem of null-filling, the aerial engineer requires to know the range of methods available, their characteristics and how they can be achieved in practice. The main features of the more important methods from which a selection would be made are summarized below.

1. Twin-Beam Method (Section 3.1.2)

(i) smooth adjustable null-filling up to 100% but individual pattern minima not independently controllable.
(ii) co-phased quarter-sine-wave amplitude distribution, with superposed pedestal for reduced null-filling.
(iii) null-filling above the horizontal contributes to the gain reduction, which is not excessive.
(iv) complex power-splitting arrangements required for realization; power division very non-uniform for high null-filling.
(v) panel-tilting not required.
(vi) good impedance and bandwidth properties since phase distribution is only required for beam-tilt.

2. Phase Perturbation (Section 3.2.1)

(i) controllable null-filling available up to 50%; difficult to reduce null-filling above the horizontal.
(ii) constant-amplitude current distribution.
(iii) reasonably low gain-reduction compatible with null-filling; adequate pattern bandwidth.
(iv) realization with simple branch-feeder system combined with limited panel-tilt where required.

3. Constant-Amplitude Stationary-Phase Method (Section 3.2.2)

(i) unlimited effective null-filling available but pattern minima uneven and not controllable individually.
(ii) suppressed v.r.p. above the horizontal.
(iii) constant-amplitude current distribution.
(iv) high gain-reductions due to elevated pattern sidelobes below the horizontal.
(v) restricted pattern bandwidth due to rather large pattern maximum-to-minimum ratios in the v.r.p.
(vi) realization with simple branch-feeder/panel-tilt arrangements.

4. General Stationary-Phase Method (Section 3.3.4)

(i) null-filling is adjustable and reasonably smooth but pattern minima not controllable individually.
(ii) variable-amplitude and variable-phase current distribution; amplitude component can be made to follow a convenient practical distribution.
(iii) pattern partially suppressed above the horizontal resulting in low gain-reduction for given null-filling.
(iv) realization possible with simple power-splitting transformers, branch-feeder systems and panel-tilting.

5. Current and Polynomial-Root Perturbation (Sections 3.3.3 and 3.3.5)

(i) null-filling very accurate and the levels of individual minima can be specified independently; null-filling completely suppressed above the horizontal.
(ii) variable-amplitude and variable-phase current distribution; phase variation is generally very small whereas the degree of amplitude variation depends on the null-filling.
(iii) offers the smallest gain-reductions of all the methods because null-filling is totally restricted to the wanted pattern region(s).
(iv) disadvantage is that realization of the current distribution requires complex power-splitting arrangements.
(v) panel-tilt is not required.

Although these methods give predictable v.r.p.s, the accuracy of null-filling should always be checked by pattern computation especially when the performance over a wide frequency bandwidth is required.

The main conclusions to be drawn can be expressed in the form of recommendations for null-filling the v.r.p.s of practical transmitting aerials; these recommendations, based on the properties and characteristics of the available design methods together with experience gained from their theoretical exploration (Sections 4.1, 4.2.2) may be summarized as follows:

(i) V.H.F. and low-power (relay) u.h.f. aerials

The method of phase perturbation, method (2), is recommended since null-filling is not normally required to be greater than 50% and the current distribution can be obtained from a simple branch-feeder system. The oscillatory solution should be used for v.h.f. and the non-oscillatory solution for u.h.f.

(ii) High-power (main station) u.h.f. aerials

(a) The preferred solution is given by the general stationary-phase method, number (4) since this gives adequate null-filling (50 to 100%) from practical amplitude distributions without undue loss of gain or greatly elevated pattern sidelobes; moreover, the phase component of the current distribution is easily realized with a branch-feeder system together with panel-tilt which can be restricted to a single end-panel. This panel-tilt is used to control the level of pattern minima at the larger declinations.

(b) The phase-perturbation method can be used with advantage if the required null-filling is not greater than about 50% over the specified range of declinations (the non-oscillatory solution is recommended).

(c) For smooth high-degree null-filling (75 to 100%) the twin-beam method must be used but the penalty paid is a complicated power-splitting arrangement and excessive gain-reduction.

In all these methods, the effects of random errors in the branch-feeder system and of errors in the actual current distribution due to inter-tier mutual coupling can be reduced to an insignificant level. With vertical impedance compensation, the aerial matching is very sensitive to beam-tilt and, in general, the matching will improve if the beam-tilt is increased. The pattern bandwidth is satisfactory with all three recommended null-filling solutions.

6. REFERENCES

1. WOODWARD, P.M., *and* LAWSON, J.D. 1948. The theoretical precision with which an arbitrary radiation-pattern may be obtained from a source of finite size. *J.Inst.elect. Engrs.*, 1948, **95**, III, 37, pp. 363 - 370.
2. WOODWARD, P.M. 1953. Probability and information theory, with applications to radar. London, Pergamon Press Ltd., 1953, p. 29.
3. DUNBAR, A.S. 1952. On the theory of beam shaping. *J.Appl.Phys.*, 1952, **23**, 8, pp. 847 - 853.
4. SHANKS, H.E. 1960. A geometrical optics method of pattern synthesis for linear arrays. *IRE Trans.Antennas Propag.*, 1960, **AP-8**, 5, pp. 485 - 490.
5. KRUPITSKIY, E.K. 1966. The synthesis of a continuous linear antenna by the stationary-phase method. *Radio Engng. and Electronic Physics* (Russian), 1966, XI, 4, pp. 559 - 566.
6. SCHELKUNOFF, S.A. 1943. A mathematical theory of linear arrays. *Bell Syst. Tech.J.*, 1943, **22**, 1, pp. 80 - 107.
7. RHODES, D.R. 1963. The optimum line source for the best mean-square approximation to a given radiation pattern. *I.E.E.E.Trans.Antennas Propag.*, 1963, **AP-11**, 4, pp. 440 - 446.
8. PROCTOR, E.K. *and* ABLOW, C.M. 1962. A variational method of synthesizing antenna power patterns. JORDAN, E.C. *ed.* Electromagnetic theory and antennas. Part 2, New York, Macmillan, 1963, pp. 1225 - 1228.
9. SILVER, S. 1949. Microwave antenna theory and design. M.I.T.Radiation Lab. Series No. 12. New York, McGraw-Hill Book Co. Inc., 1949, p. 281.
10. HILL, P.C.J. 1965. A method for synthesizing a cosecant radiation pattern by phase variation of a constant amplitude equispaced linear array. Electromagnetic Wave Theory, Oxford and New York, Pergamon, 1967, pp. 815 - 820. (Proceedings of 1965 URSI Symposium on EM Wave Theory, Delft, Netherlands).
11. Shaping the vertical radiation patterns of v.h.f. and u.h.f. transmitting aerials by phase perturbation. BBC Research Department Report No. E-121, Serial No. 1966/72.
12. A 'stationary-phase' method for shaping the vertical radiation patterns of u.h.f. transmitting aerials. BBC Research Department Report No. RA-6, Serial No. 1967/27.
13. KOHLER, K. 1963. A new method for obtaining smooth gap-filled patterns for television transmitting aerials. Rundfunktechnische Mitteilungen, 1964, **8**, 3, pp. 152 - 155.
14. WOODWARD, P.M. 1946. A method of calculating the field over a plane aperture required to produce a given polar diagram. *J.Inst.elect. Engrs.*, 1946, **93**, IIIA, 10, pp. 1554 - 1558.
15. GIHRING, H.E. 1959. 'Latest trends in TV broadcast antennas'. RCA Broadcast News, **105**, Sept. 1959, pp. 56 - 62.
16. A note on the solution of algebraic equations with complex coefficients related to aerial null-filling calculations. BBC Research Department Report No. RA-7, Serial No. 1967/36.
17. A vertically polarized transmitting aerial for u.h.f. relay stations. BBC Research Department (Confidential) Report No. E-122, Serial No. 1966/74.
18. SHONE, A.B. 1966. Impedance correction in the vertical distribution feeder system of a null-filled high gain aerial. *Electronic Engng.*, 1966, **38**, 461, July, pp. 446 - 448.

SMW

Printed by BBC Research Department, Kingswood Warren, Tadworth, Surrey